Title
POWER REAUIREMENTS FOR LIQUID AGITATION IN RECTANGULAR VESSEL

Authors
Coughlen, Thomas David
Vermeulen, Theodore.

Publication Date
1968-08-26

UCRL-16289

cy. 2

POWER REQUIREMENTS FOR LIQUID AGITATION IN RECTANGULAR VESSELS

Thomas David Coughlen and Theodore Vermeulen

August 26, 1968

LAWRENCE RADIATION LABORATORY
UNIVERSITY of CALIFORNIA BERKELEY

DISCLAIMER

UCRL-16289

UNIVERSITY OF CALIFORNIA

Lawrence Radiation Laboratory
Berkeley, California

AEC Contract No. W-7405-eng-48

POWER REQUIREMENTS FOR LIQUID AGITATION IN RECTANGULAR VESSELS

Thomas David Coughlen* and Theodore Vermeulen

August 26, 1968

*M.S. thesis

POWER REQUIREMENTS FOR LIQUID AGITATION IN RECTANGULAR VESSELS

Contents

POWER REQUIREMENTS FOR LIQUID AGITATION IN RECTANGULAR VESSELS

Thomas David Coughlen and Theodore Vermeulen

Lawrence Radiation Laboratory and Department of Chemical Engineering
University of California
Berkeley, California

August 26, 1968

ABSTRACT

Power requirements have been investigated for liquid agitation in a closed rectangular tank having variable cross-section, using both four-bladed flat paddles and flat-bladed turbines with a varying number of blades. For three rectangular cross-sections studied, the power-speed relations lie between those for unbaffled and for fully baffled cylindrical tanks. In correlating the experimental data, a dimensionless power number which includes the impeller length-to-width ratio to the first power is found useful. For runs with flat-bladed turbines, the maximum power input at any given rotor speed is produced by turbines with around 12 blades. Air-water mixtures agitated with a four-bladed flat paddle showed greater percentage reductions in power requirement for the cross-sections exhibiting the higher air-free power inputs.

I. INTRODUCTION

Mixing comprises a group of operations concerned with the internal movement of bodies of fluid (or particulate solid) so as to reduce non-uniformities or gradients in composition, temperature, or other bulk properties of the material involved. The movement of fluids occurs by a combination of bulk flow (in either laminar or turbulent regimes) and eddy and molecular diffusion. To accomplish all but molecular diffusion, energy must be added to the system. A common method of introducing energy, the one of interest in the present study, is by a rotating impeller inserted in a body of fluid.

The present work examines the energy-input or power requirements in square and rectangular closed vessels using agitators of different geometrical designs. To understand better the effects of vessel geometry, comparison is made between the vessels studied and both baffled and unbaffled cylindrical vessels. Also, correlations of agitator geometry are developed that will aid in the future design and selection of agitators.

Power requirements have long been the topic of agitation studies. Early investigators (W1) used rectangular wooden paddles, with a torsion dynamometer to measure the power input. Hixson and Baum (H2) employed flat paddles, with the blades mounted at 45°, 60°, and 90°, to correlate power requirements, while Olney and Carlson (O2) used arrowhead impellers and spiral turbines. A comprehensive investigation by Rushton, Costich, and Everett (R2) included propellers, arrowhead turbines, flat-bladed turbines, curved-bladed turbines, shrouded turbines, and flat paddles.

Mack (M1) estimated agitator power requirements for flat-bladed turbines having from two to sixteen blades and having impeller length-to-width ratios from two to twelve. Rushton, Costich, and Everett (R2) presented the mathematical approach to the development of three dimensionless terms, the impeller Reynolds number $N_{Re}=N\ L^2\rho\ /\mu$, the Froude number $N_{Fr}= L\ N^2/g$, and the power number $P_o = Pg_c/(N^3L^5\rho)$, where N is the impeller speed, L the impeller diameter, ρ the fluid density, μ the fluid viscosity, g the gravitational acceleration, g_c the conversion factor between force and mass, and P the power input to the system.

The Reynolds number represents the ratio of inertial forces to viscous forces and is the parameter generally chosen for the correlation of the power number when viscous forces are dominate. Work by Hinze (H1), Shinnar and Church (S1), and others, based on Kolmogorov's statistical theory of turbulence, suggests the use of a dimensionless group based on power input per unit mass, the cube of the kinematic viscosity, and a characteristic length: $\epsilon d^4\ /\nu^3$. However, the power behavior for turbulently agitated vessels (except for geometric factors) is usually given by

$$\epsilon \propto N^3\ d^2 \qquad (1)$$

Hence the power-dissipation group is essentially the cube of the Reynolds group.

The Froude number represents the ratio of inertial to gravitational forces, and would be expected to be a factor in unbaffled tanks, where swirl combines with gravitational forces to control the motion. However,

Nagata and Yokoyama (N4) have found that the correction for Froude number in unbaffled tanks is negligible.

Variations in geometry can be correlated as a matter of convenience, but Bates, Fondy, and Fenic (B1) correctly comment that there is as yet no theoretical basis for doing so.

Baffling has the effect of preventing swirl and vortex formation, allowing more power to be delivered to a system at a given impeller speed than in unbaffled conditions. In the laminar-flow regime, baffling has no effect (R2). Baffles alter the flow pattern from an unbaffled cylindrical tank by greatly decreasing the tangential fluid velocity and increasing the radial and axial fluid velocities, thereby greatly increasing the momentum-transfer rate. The constantly varying distances between the impeller tip and the wall in square and rectangular cross-sections should have some baffling action. To eliminate or reduce swirl, an alternate to baffling is off-center mounting of the impeller, a method used primarily for axial-flow (propeller) systems.

In a closed tank completely filled with liquid, vortexing is impossible, but, as in part of this study, when a portion of the liquid in a closed vessel is replaced with air, two-phase mixing occurs. For agitation of gas-liquid mixtures, little effort has been made to explain the large reduction in power that accompanies the introduction of gas into the agitated liquid system, although several investigators have measured power requirements. Clark and Vermeulen (C1) bubbled gas through a liquid mixing system and correlated the power number using the Froude number, the impeller-to-tank-volume ratio, and the effect of impeller

depth. The mechanism whereby gas from above is introduced into a liquid agitated in a baffled tank was also explored. The flow pattern responsible for the introduction of air into this liquid had been reported previously by Taylor and Metzner (T1,M2).

This study uses closed vessels with square and rectangular cross-sections to examine power requirements for liquid and liquid-air systems. Two different types of impellers are used; the flat-bladed paddle to determine the effects of paddle length and width; and the flat-bladed disk turbine to correlate the number of blades. The results are compared with both baffled and unbaffled cylindrical tanks and a discussion of the differences is presented.

II. THEORY

A. MIXING PROCESSES

In any system of two kinds of molecules, given enough time, molecular diffusion will occur and cause a uniform mixture to form. If turbulence can be generated, the eddy diffusion effects will accelerate the mass-transfer process. The turbulent process can be used to break up fluid elements into smaller clumps, down to a limiting range where molecular diffusion begins, across the boundary areas between clumps, to control the rate of homogenization or equilibration. On a still larger scale, agitation produces a relative bulk motion between different masses of fluid, which increases their accessibility for structural disintegration by the turbulence which also results from the overall agitation. (B2)

B. IMPELLER DISCHARGE RATES - THEORETICAL RELATIONSHIP

The first section describes what takes place in a moving fluid when concentration or property differences are present. Mixing is considered to be a process in which progressively greater uniformity is obtained as a result of various types of fluid motion, such as laminar flow, turbulent flow, and molecular diffusion.

Flow within a vessel is caused by the interaction of the impeller with the liquid. The resultant discharge velocities and discharge flow rates depend upon the geometry of the vessel and the impeller. Gray (G1) presents theoretical relationships for the curved-blade turbine of which the flat-bladed turbine is a special case where α is zero. In Fig. 1 the velocity vectors at the periphery of a curved-blade turbine impeller are shown and the terms defined.

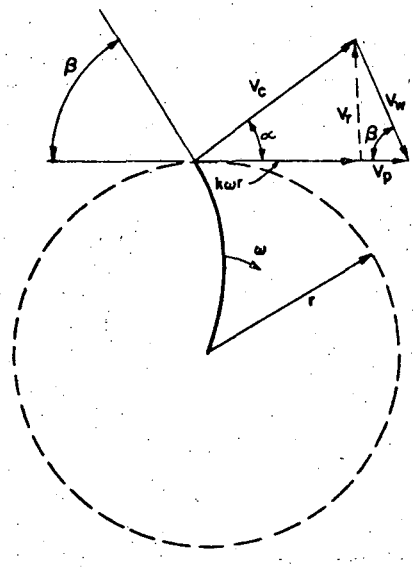

k = ratio of tangential fluid velocity at the periphery of an impeller to the peripheral impeller velocity,

r = radial distance from center of rotation, ft.,

v_c = fluid velocity leaving the periphery of an impeller, ft./min.,

v_p = peripheral impeller velocity, ft./min.,

v_r = radial velocity component, ft./min.,

v_w = fluid velocity relative to impeller blade tip, ft./min.,

α = angle between velocity vectors, v_c and v_p,

β = angle between impeller tip and velocity vector, v_p,

ω = angular velocity, radians/min.

Fig. 1. Discharge velocity for a curved-blade turbine (G1).

Based on an angular-momentum balance the author derives an equation relating the velocities and theoretical head developed by a rotating impeller. The time rate of change of angular momentum of the fluid passing through the impeller is equal to the torque or moment of the forces applied to the fluid by the impeller surfaces. If the angular momentum of the fluid entering the impeller is assumed to be zero, and the fluid friction losses are assumed to be zero, the power can be expressed as follows:

$$P = Q\rho H \qquad (2)$$

Where H is the theoretical impeller head, P the power, Q the impeller discharge rate, and ρ the fluid density. When there are no friction losses in the impeller theoretical head, H can also be expressed in terms of the kinetic head, $V_c^2/2g_c$, and the static head that is due to centrifugal force on the liquid at the impeller periphery, $(kwr)^2/2g_c$ or

$$H = V_c^2/2g_c + (kwr)^2/2g_c \qquad (3)$$

Using these equations and others that can be written from inspection of the diagram in Fig. 1, Gray shows that k, α and β are not independent.

The radial pumping capacity of an impeller in an agitated vessel is calculated from the following equation:

$$Q = 2\pi WrV_r \qquad (4)$$

where W = the axial impeller blade width. A dimensionless impeller-discharge coefficient is defined thus:

$$N_Q = Q/NL^3 \qquad (5)$$

where L is the impeller diameter and N the impeller rotational speed. By substitution, relationships for the discharge rate, Q, and the impeller discharge coefficient in terms of the impeller rotational speed, the geometry of the impeller, and k, the ratio of the tangential fluid velocity at the periphery of an impeller to the peripheral impeller velocity can be expressed as such,

$$Q = \pi^2 WNL^2\ 2k(1-k) \tag{6}$$

$$N_Q = \pi^2 (W/L)\ 2k(1-k) \tag{7}$$

The following derived relationship is independent of the type of impeller:

$$N_Q = P_o/\pi^2\ k \tag{8}$$

Zero friction losses were assumed for fluid passing through an impeller and the fluid entering the impeller was assumed to be not rotating. From equation (8) values of k can be calculated from power and impeller-discharge experimental data.

Equation (6) must be modified when applied to impellers in agitated vessels because (a) the flow from actual impellers is distorted by the use of relatively few blades or vanes, (b) part of the kinetic and static heads is dissipated by turbulent motion and viscous drag, and (c) the fluid does not have zero rotational velocity entering the impeller unless the vessel is baffled.

C. FLUID VELOCITY COMPONENTS - EXPERIMENTAL RESULTS

Nagata et al (N_1, N_2, N_3) have studied velocities, flow rates, and flow patterns for various rotating impellers in both baffled and unbaffled circular vessels, with the impellers located halfway between the liquid

surface (open top) and the bottom of the vessel. The Reynolds number was varied from 10 to 10^5. Fluid directions and corresponding velocities were obtained only for the upper half of the vessel. Velocities in the lower half were assumed to be similar to those in the upper half. It is useful to summarize their findings here.

As expected, for an unbaffled vessel, the tangential-velocity component is high relative to radial and axial components, and is proportional to the distance from the center of the agitator shaft throughout the region above and below the rotating impeller. This component attains a peak value just inside the outer edge of the turbine blade, then diminishes at an almost constant rate, leveling off near the vessel wall. The behavior at the wall boundary was not indicated. Radial velocity components are directed toward the shaft, everywhere except at the level of the impeller where they are toward the vessel wall. Beginning at the impeller tip there are two lines that begin just to the inside of the upper and lower horizontal edges of the impeller and that slowly diverge toward the vessel wall where the radial velocity is zero. The axial velocity component (parallel to the shaft) returns to the impeller in an annulus around the shaft and in a torus above and below the outer edge of the impeller as shown in Figure 2. Near the vessel wall and in the region above the horizontal midplane of the impeller the fluid moves away from the impeller.

The effect of adding eight evenly spaced baffles, each one-thirteenth of the tank diameter, was determined under turbulent-flow conditions. The flow pattern is more erratic with baffles than without baffles. The insertion

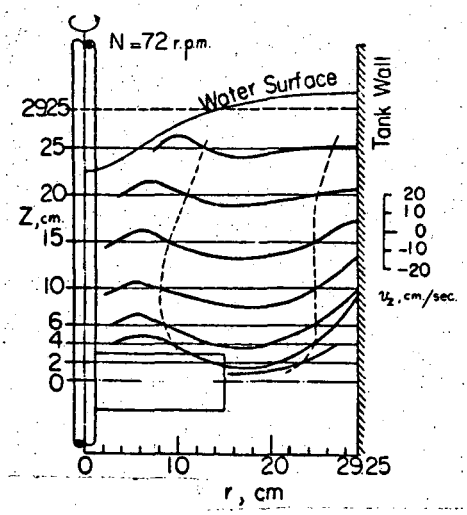

Fig. 2. Axial velocities produced by a 16-flat-blade paddle in an unbaffled vessel at 72 r.p.m. Paddle is located halfway between the water surface and the bottom of the vessel (N3).

of baffles greatly decreases the tangential velocities, while both radial and axial velocities are increased. At one location inside the agitator periphery the tangential flow direction is opposite to that of the impeller rotation. Nagata et al. attributed the reverse flow to eddies caused by tangential flow past the baffle plates. Near the tank wall and the baffle plates these eddies die out rapidly, but near the shaft they induce a smaller, more stable eddy.

Radial velocities are directed toward the wall in a much larger region in baffled vessels than in unbaffled ones. For the impeller studied, this region extended from a distance of three impeller widths along the impeller edge to six impeller widths at the tank wall. Axial velocities were directed away from the agitator in the area near the vessel wall, and toward the agitator in the rest of the vessel.

Nagata et al. indicated the water surface to be flat for baffled turbulent conditions. For unbaffled mixing, the fluid level was higher in the outer half of the vessel, causing a widely encountered depression or "vortex" around the shaft which is intensified by the high tangential velocities in this region. Thus, in unbaffled vessels, the maximum power input occurs at the speed where vortexing begins.

III. EXPERIMENTAL PROGRAM

A. PHYSICAL VARIABLES INVOLVED

The variables considered in this study are as follows:

(1) Volume-fraction of the gas or dispersed phase,

(2) Physical properties of the agitated fluids,

(3) Impeller speed,

(4) Vessel geometry; shape and dimensions,

(5) Impeller geometry:

Flat-bladed turbine: number of blades,

Flat-bladed paddle: blade length (diameter) and blade width.

By using a closed vessel, it was possible to vary the amount of liquid so as to obtain liquid/air mixtures where the volume-fraction of the dispersed gas phase ranged from 0 to 15 percent. The choice of liquids used and the range of impeller speeds yielded N_{Re} from the transition to the fully turbulent zone (200 to 200,000).

In this study emphasis has been placed on the geometrical variables. Square and rectangular cross-sections have been measured, and are compared to results obtained in earlier studies on unbaffled and fully baffled vessels of circular cross-section. The number of blades of a flat-bladed turbine has been varied in relation to power input. The parameters for flat-bladed paddles have been impeller length (diameter), width, and impeller length to width ratio. The impeller drive mechanism produced three constant rotational speeds (155, 247, and 396 rpm).

B. SYSTEMS INVESTIGATED

The liquids used in this study are listed in Table I along with pertinent physical properties.

TABLE I. PHYSICAL PROPERTIES OF LIQUIDS USED IN MIXING STUDIES

Liquid	Density lb/ft^3	Viscosity lb/ft.sec
Aqueous glycerol solution (68.71 wt.% glycerol)	73.53	0.01384
water (distilled)	62.32	0.0006733
white oil	53.94	0.1304

(1) All properties at 20° ± 0.5°C.

C. APPARATUS

The mixing vessel was a cubic stainless steel tank, approximately ten inches in inside length, width, and height, with a fixed impeller. Insertion of flat 1/16-inch-thick "divider" panels in the positions shown in Figure 3 enabled the geometry of the rectangular cross-section to be varied. Cross-sections studied were square, with impeller centered, (no dividers); rectangular, with impeller centered (both dividers inserted); and rectangular, with impeller off-center (one divider inserted).

The dividers fit snugly into rectangular grooves in the sides and bottom of the tank. To prevent exchange of fluid between the compartments, gaskets were inserted between the dividers and the top and bottom of the tank; at the bottom a 1/16-inch square strip of silicone rubber; at the top, slit-open neoprene tubing, fitted over the top edge of the divider plate.

Although the divided compartments are not mutually liquid or air-tight, it was noted that immediately following a baffled air-white oil run, the agitated white oil contained a sizeable amount of suspended air, while the white oil in the isolated compartments showed no sign of suspended air.

The tank was attached to a frame constructed of five-inch channel iron, by means of an integral-suspension ball-bearing unit welded to the tank cover. A collar welded to the upper side of the frame, aligned axially with the tank-cover assembly, contained a ball bearing spindle assembly to which the impeller shaft was connected; in the latter, two sets of ball bearings were located as far apart as possible, so as to minimize any whip from the impeller. The final assembly of these units permitted

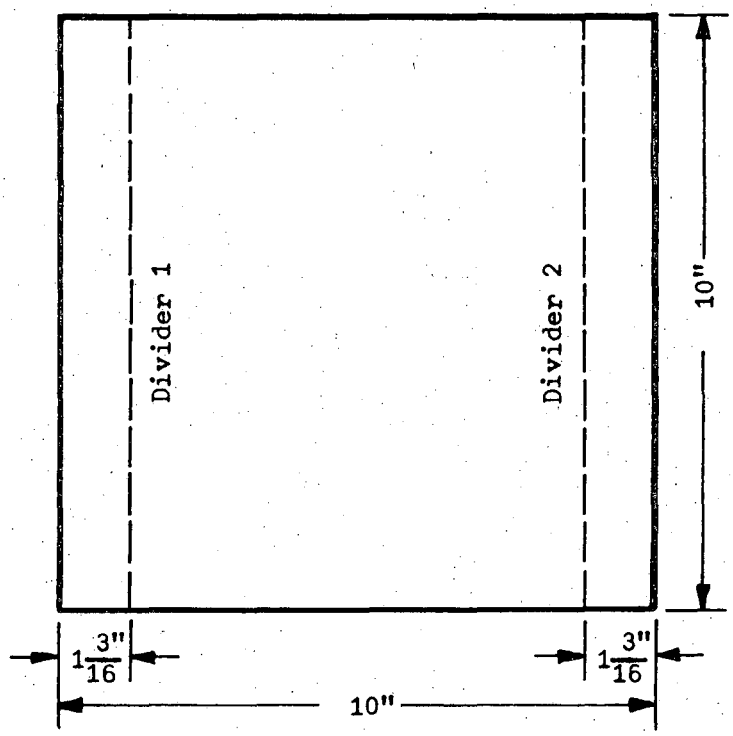

Fig. 3. Top view of tank showing divider positions.

XBL 6810-6093

free rotation of the tank cover assembly and the impeller shaft, each independent of the other, thereby enabling the power required in mixing to be determined by torque measurements. The tank assembly is shown in Figure 4.

The tank proper was fastened to the tank cover by a circle of bolts and wing nuts. A 1/16-inch silicone-rubber gasket was placed between the flanged edge of the tank and the cover to provide a leakproof fit. A mercury seal was used to make the impeller shaft liquid-and-air-tight.

The tank cover contained several openings; these were capped or plugged during the experiments, except for a thermometer well fitted with silicone gaskets to provide a tight seal. A 1/2-inch pipe outlet in the center of the tank bottom was also plugged during the runs. A 30-foot long coil of 1/4-inch o.d. copper tubing was soldered to the outside of the tank to provide circulation of cooling water for temperature control of the tank contents.

Flat-bladed paddles and turbines were used as agitators. Figure 5 shows a diagram and the dimensions of the four-bladed flat paddles; they varied in diameter through a factor of 1.5, in width through a factor of 2, and in diameter-to-width ratio (L/W) through a factor of 3. Figure 6 shows a diagram of a flat-bladed turbine with four blades. Turbines of identical diameter and blade width, with two, four, six and eight blades were used, the dimensions in each case being as shown in Figure 6.

All impellers were driven by means of a V-belt drive connected to a 3/4-horsepower 3-phase, 60-cycle, 220 volt, 216 rpm right angle ring-mounted

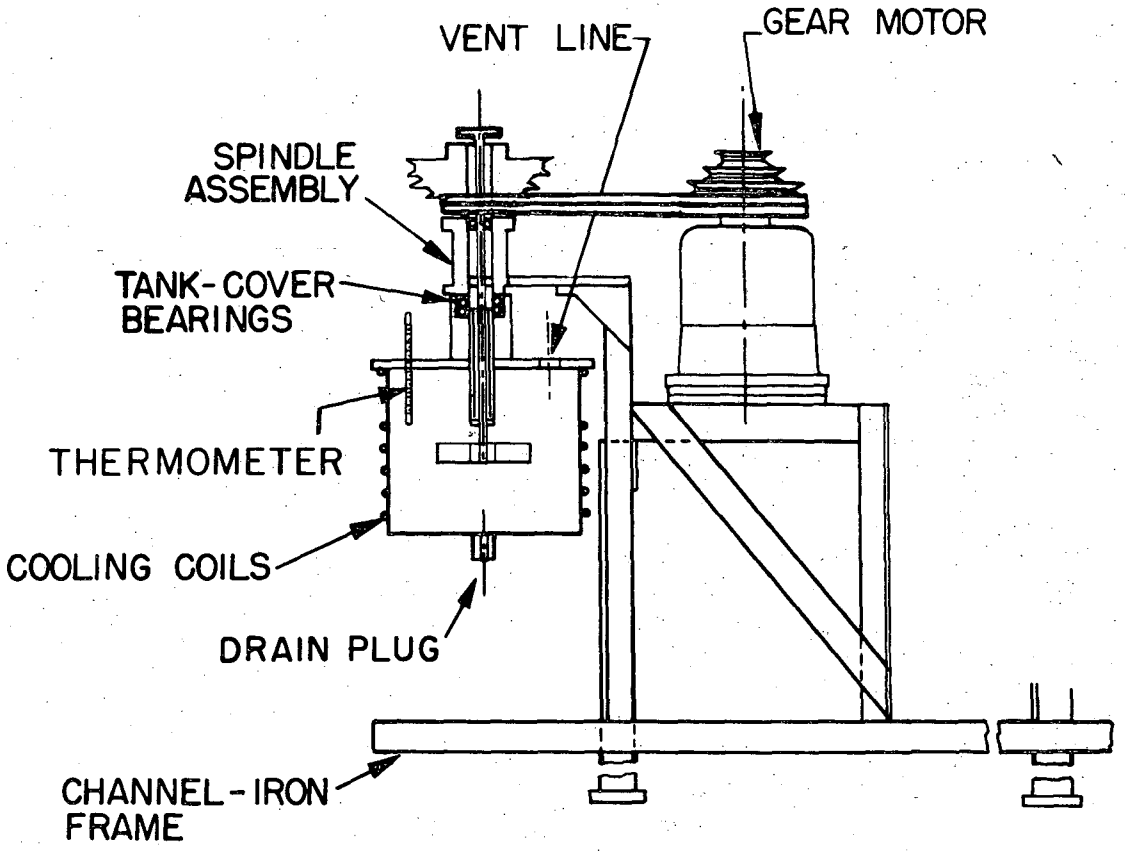

XBL 6810-6094

Fig. 4. Tank and motor assembly.

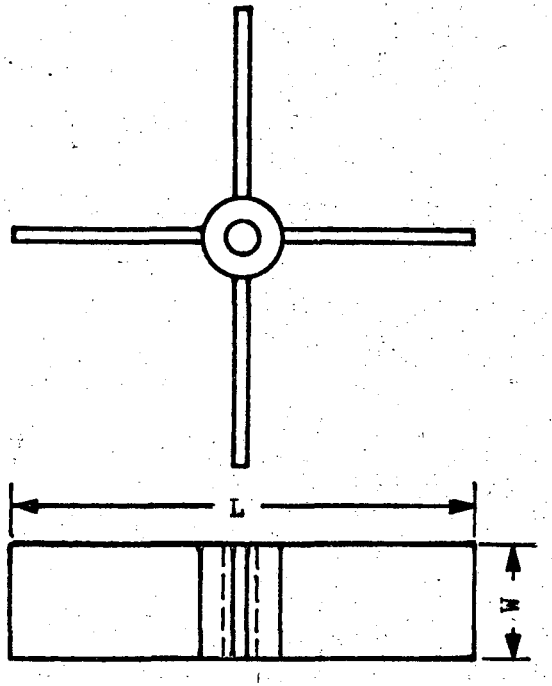

Paddle	L	W	L/W
A-2	4.98	0.98	5.08
A-3	7.47	0.97	7.70
A-4	6.73	1.64	4.10
A-5	4.99	1.98	2.52

Fig. 5. Four bladed flat paddles (dimensions in inches).

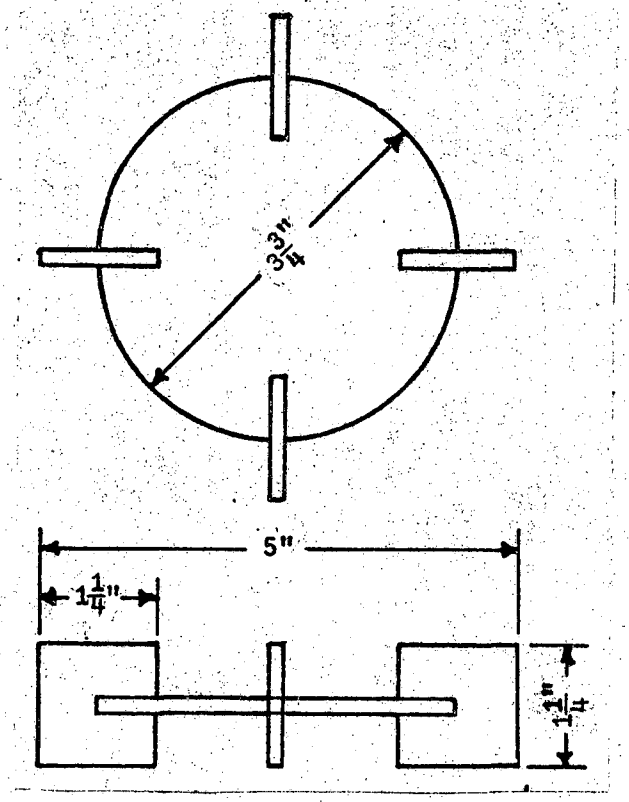

Fig. 6. Blade-and-disk turbine dimensions.
Turbine R-0, 2 blades; R-1, 4 blades; R-2, 6 blades; R-3, 8 blades.

gear motor supplied by Electra Motors, Inc. The V step-cone pulley arrangement allowed the impellers to rotate at 155, 247, and 396 rpm.

Power requirements in the system studied were measured by using the tank as part of a dynamometer. Ten-thousandths-inch-diameter stainless steel wire was attached to the tank collar, and led through a nearly frictionless pulley. Attached to the other end of the wire was a variable weighted platform which rested on one pan of a Toledo Scale, Model 4021 BA, a double-pan model. The force necessary to hold the tank stationary during impeller rotation could be measured by observing the changes in scale readings, which were generally reproducible within an average of $\pm$ 1.0 per cent of the total force. Experiments with the tank empty indicated that the mercury seal produced negligible torque.

D. OPERATING PROCEDURE

In preparation for a run, the tank and associated equipment were thoroughly cleaned, and then rinsed with the liquids to be used. The tank was then charged with the liquid under investigation; when its temperature reached 20 $\pm$ 0.5°C, the thermometer was withdrawn, the liquid level checked and adjusted if necessary, the thermometer reinserted, and cooling hoses detached to permit the tank to revolve freely.

For each impeller, power readings were recorded at all speeds. Runs were made in which the impellers were changed while keeping the same tank shape, and in which the same impeller was used while varying the tank shape. The sequence of impeller speeds or operating conditions used had no effect on the power reading.

The weight platform contained a series of weights sufficiently greater than the force expected in order that the platform would remain firmly on the scale pan. Weights as necessary were added to the opposing pan to bring the power reading within the range of the balance-scale. The force readings showed rapid fluctuation, that were very slight at low speeds but reached approximately 3 per cent at the highest speed. More viscous fluids produced less intense fluctuations at any given speed. When fluctuations occurred, the power reading was observed over a period of time, to establish the average reading. In runs with a balancing force of less than one pound, a pseudo equilibrium range was observed, for which the extreme values of force (approached from above and from below) were averaged to determine the power reading. (In future studies the bearing friction that produced the pseudo-equilibrium range could probably be reduced by installing a thrust-bearing ring beneath the tank, and by use of nylon monofilament line instead of stainless wire.)

In all cases the accelerational or decelerational approach to steady state for the power readings was too fast to observe.

Measurements of the physical properties of the liquids were made periodically throughout the experiment, to ensure uniformity. Density measurements were made in a Westphal balance with an accuracy of 0.001 gram. Viscosity values for water and for glycerol-water solution were taken from the Handbook of Chemistry and Physics. Viscosity measurements for white oil were made from a Saybolt Fural Viscometer.

All measurements were made at 20 $\pm$ 0.5°C.

IV. RESULTS AND DISCUSSION

Besides various ratios of other geometrical dimensions to the impeller diameter, the expression for the power number given by Buckingham's Pi Theorem has one dimensionless number to account for the number of impeller blades, and two standard dimensionless groups for liquid flow, the Reynolds number and the Froude number. (B1) It can be written in the form

$$P = K(N_{Re})^a (N_{Fr})^b \left(\frac{T}{L}\right)^c \left(\frac{Z}{L}\right)^d \left(\frac{C}{L}\right)^e \left(\frac{p}{L}\right)^f \left(\frac{W}{L}\right)^g \left(\frac{l}{L}\right)^h \left(\frac{n_1}{n_2}\right)^i \quad (9)$$

where

P_o = power number = $Pg_c/(\rho N^3 L^5)$, (10)

N_{Re} = Reynolds number = $NL^2\rho/\mu$, (11)

N_{Fr} = Froude number = LN^2/g, (12)

C = clearance of impeller off vessel bottom,

K = constant,

L = impeller diameter,

N = impeller rotational speed,

P = power,

T = tank diameter,

W = impeller width,

Z = liquid depth,

g = gravitational acceleration,

g_c = conversion factor between force and mass,

l = blade length,

n = number of blades,

p = pitch of blades,

μ = liquid viscosity,

ρ = liquid density,

all in consistent units.

The Reynolds number represents the ratio of inertial forces to viscous forces, and determines whether the flow is laminar or turbulent. The Froude number represents the ratio of inertial to gravitational forces and could be an influencing factor where vortexing occurs in an open vessel with a free liquid surface. The power number is a measure of the "pressure coefficient" and represents the ratio of pressure differences producing flow to inertial forces.

Gravitational effects are generally considered to be unimportant for baffled tanks and for laminar mixing. Nagata and Yokoyama (N4) obtained good correlations between P_o and N_{Re} in unbaffled tanks without using N_{Fr} and stated that the correction for the Froude number was negligible.

When two systems are geometrically similar, dynamic similarity exists when the ratios of all corresponding forces are equal. Kinematic similarity occurs when velocities at corresponding points are in the same ratio.

The exponents of the dimensionless groups in equation (9) are not constant throughout the range from laminar to turbulent and in the general case can depend upon all of the dimensionless variables. The effect of one geometric variable on a system can be studied if all other parameters are held constant. It would be improper to use one of the groups to modify the power number for the general case. But for a given set of conditions, the interaction of a group, say $(W/L)^g$, with N_{Re} could be studied by varying W/L experimentally at Reynolds numbers in the fully turbulent regime where the flow pattern is reasonably independent of Reynolds number. The effect determined would be expected to be constant within the regime.

A. EXPERIMENTAL RESULTS

1. Single - Phase Data

Four-Bladed Flat Paddles

Experimental runs were made with the flat-bladed paddles using water, white oil and a glycerin-water solution in a closed tank for three cross-sections: square (impeller centered), rectangular (impeller off-center), and rectangular (impeller centered), at impeller speeds of 2.58, 4.12, and 6.59 revolutions per second. Table II shows the experimental data, along with certain calculations made from the data. For each run the table lists the force on the lever arm and the corresponding power consumed by the system. Equations (10) and (11) were used to calculate the resulting power number, P_o, and Reynolds number, N_{Re}. Also included is the modified power number

$$P_w = P_o(L/W)^{1.0} = P g_c/(\rho N^3 L^4 W) \qquad (13)$$

which introduces the effect of impeller width into the power number, P_o, so that paddles with varying lengths and widths can be correlated. Part B of this section discusses the reasons for using 1.0 as the value for the exponent of the ratio L/W.

Paddle A-2(L = 4.98", W = 0.98") and paddle A-5 (L = 4.99", W = 1.98") have the same length, and power requirements can be compared to determine the effect of blade width. Reynolds number is a function of impeller diameter, not of impeller width, and N_{Re} for the two impellers is then the same for a given liquid at a specified rotational speed. Since all other conditions are the same, the effect of blade width upon power consumption can be determined from the exponent x in the following relationship:

TABLE II. POWER CONSUMPTION FOR FLAT-BLADED PADDLES IN SINGLE-PHASE SYSTEMS

Cross-Section	System	Impeller No	N revs/sec	Force on lever arm, lb.	P Horse-power	P_o Dimen-sionless	P_w Dimen-sionless	N_{Re} Dimen-sionless
Square	Water	A-2	4.12	0.85	0.06962	1.913	9.718	65,670
			6.59	2.18	0.2851	1.917	9.738	105,060
		A-3	4.12	4.00	0.3276	1.186	9.132	147,700
			6.59	9.98	1.305	1.156	8.901	236,400
		A-4	2.58	1.51	0.07745	1.922	7.880	75,100
			4.12	3.74	0.3063	1.868	7.659	120,000
			6.59	9.48	1.240	1.850	7.585	191,900
		A-5	2.58	0.55	0.02821	3.090	7.787	41,290
			4.12	1.24	0.1016	2.827	7.124	65,940
			6.59	2.98	0.3898	2.594	6.537	105,500
Square	Glycerin-Water	A-2	2.58	0.54	0.01707	2.624	13.35	2,362
			4.12	1.29	0.1056	2.462	12.51	3,772
			6.59	3.30	0.4316	2.458	12.49	6,034
		A-3	2.58	2.56	0.08092	1.640	12.63	5,315
			4.12	6.03	0.4938	1.516	11.67	8,484
			6.59	14.04	1.836	1.379	10.62	13,580
		A-4	2.58	2.48	0.07839	2.678	10.99	4,313
			4.12	5.93	0.4857	2.511	10.30	6,890
			6.59	14.05	1.838	2.326	9.543	11,010
		A-5	2.58	0.97	0.03066	4.671	11.77	2,371
			4.12	2.31	0.1892	4.365	11.00	3,787
			6.59	5.34	0.6985	3.942	9.934	6,060
Square	White Oil	A-2	4.12	1.04	0.08518	2.705	13.74	293.4
			6.59	2.97	0.3885	3.018	15.33	469.4
		A-3	2.58	1.99	0.06290	1.738	13.38	413.5
			4.12	5.12	0.4193	1.754	13.50	660.1
			6.59	12.63	1.652	1.690	13.01	1,056

TABLE II. (2)

Cross-Section	System	Impeller No.	N revs/sec	Force on Lever arm, lb.	P Horse-power	P_o Dimen-sionless	P_w Dimen-sionless	N_{Re} Dimen-sionless
Square	White Oil	A-4	2.58	2.50	0.07902	3.678	15.08	335.6
			4.12	5.78	0.4734	3.336	13.68	536.0
			6.59	14.18	1.855	3.198	13.11	857.0
		A-5	2.58	0.91	0.02876	5.973	15.05	184.5
			4.12	2.40	0.1966	6.180	15.57	294.6
			6.59	5.98	0.7822	6.016	15.16	471.5
Rectangular, Off-Center	Water	A-2	2.58	0.33	0.01692	1.892	9.635	41,120.
			4.12	0.94	0.07699	2.116	10.75	65,670.
			6.59	2.50	0.3270	2.199	11.17	105,060.
		A-3	2.58	1.82	0.09335	1.375	10.59	92,540.
			4.12	4.69	0.3841	1.390	10.70	147,700.
			6.59	11.97	1.566	1.386	10.67	236,400.
		A-4	2.58	1.62	0.08309	2.062	8.454	75,100.
			4.12	4.12	0.3374	2.057	8.433	120,000.
			6.59	10.32	1.350	2.014	8.257	191,900.
		A-5	2.58	0.62	0.03180	3.483	8.777	41,290.
			4.12	1.54	0.1262	3.511	8.848	65,940.
			6.59	3.95	0.5167	3.439	8.666	105,500.
Rectangular, Off-Center	Glycerine-Water	A-2	2.58	0.63	0.01991	3.064	15.57	2,362.
			4.12	1.45	0.1188	2.767	14.06	3,772.
			6.59	3.49	0.4565	2.600	13.21	6,034.
		A-3	2.58	2.77	0.08756	1.774	13.66	5,315.
			4.12	6.90	0.5651	1.734	13.35	8,484.
			6.59	17.52	2.292	1.721	13.25	13,580.
		A-4	2.58	2.51	0.07934	2.710	11.12	4,313.
			4.12	6.28	0.5143	2.660	10.91	6,890.
			6.59	15.33	2.005	2.538	10.41	11,010.

TABLE II. (3)

Cross-Section	System	Impeller No.	N revs/sec	Force on lever arm, lb.	P Horse-power	P_o Dimen-sionless	P_w Dimen-sionless	N_{Re} Dimen-sionless
Rectangular, Off-Center	Glycerine-Water	A-5	2.58	1.08	0.03414	5.200	13.11	2,371.
			4.12	2.53	0.2066	4.782	12.05	3,787.
			6.59	6.10	0.7979	4.503	11.35	6,060.
Rectangular, Off-Center	White Oil	A-2	2.58	0.49	0.01549	3.249	16.50	183.8
			4.12	1.22	0.09992	3.173	16.12	293.4
			6.59	3.05	0.3989	3.099	15.74	469.4
		A-3	2.58	2.06	0.06512	1.799	13.85	413.5
			4.12	5.14	0.4210	1.760	13.55	660.1
			6.59	12.58	1.645	1.683	12.96	1,056.
		A-4	2.58	2.46	0.07776	3.619	14.84	335.6
			4.12	6.04	0.4947	3.486	14.29	536.0
			6.59	14.75	1.929	3.333	13.66	857.0
		A-5	2.58	0.94	0.02971	6.170	15.55	184.5
			4.12	2.44	0.1998	6.283	15.83	294.6
			6.59	5.78	0.756	5.815	14.65	471.5
Rectangular Centered	Water	A-2	2.58	0.62	0.03180	3.556	18.06	41,120.
			4.12	1.56	0.1278	3.511	17.84	65,670.
			6.59	3.98	0.5206	3.500	17.78	105,060.
		A-4	2.58	2.81	0.1441	3.576	14.66	75,100.
			4.12	7.04	0.5766	3.515	14.41	120,000.
			6.59	17.45	2.284	3.405	13.96	191,900.
		A-5	2.58	1.18	0.06052	6.629	16.70	41,290.
			4.12	3.45	0.2826	7.866	19.82	65,940.
			6.59	7.73	1.011	6.730	16.96	105,500.
Rectangular Centered	Glycerine Water	A-2	2.58	0.57	0.01802	2.771	14.08	2,362.
			4.12	1.40	0.1147	2.673	13.58	3,772.
			6.59	3.44	0.4500	2.562	13.02	6,034.

TABLE II. (4)

Cross-Section	System	Impeller No.	N revs/sec	Force on lever arm, lb.	P Horse-power	P_q Dimen-sionless	P_w Dimen-sionless	N_{Re} Dimen-sionless
Rectangular Centered	Glycerine-Water	A-3	2.58	2.53	0.07997	1.622	12.48	5,315
			4.12	6.68	0.5471	1.679	12.93	8,484
			6.59	16.78	2.195	1.648	12.69	13,580
		A-4	2.58	3.00	0.09483	3.239	13.29	4,313
			4.12	7.91	0.6478	3.349	13.74	6,890
			6.59	20.20	2.642	3.344	13.72	11,010
		A-5	2.58	1.01	0.03193	4.868	12.26	2,371
			4.12	2.44	0.1998	4.611	11.62	3,787
			6.59	5.68	0.7429	4.192	10.56	6,060
Rectangular Centered	White Oil	A-2	4.12	1.12	0.09173	2.913	14.80	293.4
			6.59	2.91	0.3806	2.957	15.02	469.4
		A-4	2.58	2.42	0.07650	3.560	14.60	335.6
			4.12	6.12	0.5012	3.532	14.48	536.0
			6.59	14.91	1.949	3.362	13.78	857.0
		A-5	2.58	0.97	0.03066	6.367	16.44	184.5
			4.12	2.44	0.1998	6.283	15.83	294.6
			6.59	6.07	0.7940	6.106	15.39	471.5

$$(W_{A-5}/W_{A-2})^x = (2.02)^x = P_{A-5}/P_{A-2} \qquad (14)$$

Values of x are set forth in Table III. Overall, x varies from 0.50 to 1.10. In the transition reqion, cross-section has very little effect on x; (for white oil, x = 0.95 to 1.10, and for glycerin-water, x = 0.77 to 0.79). For the turbulent regime (water), x increases from 0.50 to 0.76 to 1.01 as the three cross-sections increase in baffling effect, the baffling effect being determined by an analysis of the flow patterns based on the values of P_w as discussed in part B. The value of x = 1.01 for the rectangular, impeller centered, cross-section was the only condition where the mixing system fell in the turbulent, fully baffled regime.

Power requirements for paddle A-2 (L = 4.98", W = 0.98") and paddle A-3 (L = 7.47", W = 0.97") can be used to look at the general effect of impeller diameter, L. Because Reynolds number is a function of impeller diameter, the values of N_{Re} will be different for like systems with the same rotational speed. Therefore, the power consumption cannot be directly compared except for fully baffled systems in the turbulent regime where the power number, P_o, is independent of N_{Re}. Paddle A-3 did not have proper clearance with both dividers inserted, and data could not be attained for paddle A-3 in the turbulent region for the cross-section that produced characteristics similar to a baffled cylindrical tank. The other two cross-sections behaved similarly to an unbaffled tank in that P_o decreased at a steady, gradual rate with increased N_{Re}. For the data taken for paddle A-3, values for the exponent y in the expression

$$(L_{A-3}/L_{A-2})^y = (1.50)^y = P_{A-3}/P_{A-2} \qquad (15)$$

ranged from 3.53 to 4.02 and averaged 3.78.

Table III. Determination of the effect of blade width on power for flat-bladed paddles A-2 and A-5. Tabulated values are for the exponent x in the relationship $(W_{A-5}/W_{A-2})^x = P_{A-5}/P_{A-2}$

System	Vessel Cross-section		
	Square	Rectangular Off-Center	Rectangular Centered
White Oil	1.10	0.95	1.08
Glycerin — Water	0.79	0.79	0.77
Water	0.50	0.76	1.01

As anticipated, the power number P_o for the different paddles increased as the W/L ratio increased. Exceptions were values of P_o for paddles A-2(W/L = 0.197) and A-4 (W/L = 0.244) which were almost the same for the three systems in the turbulent region (A-4 being 0.7 to 1.8% higher) and for two of six systems in the transition region between laminar and turbulent flow (A-4 being 0.4 and 6.2% higher). Increasing N_{Re} lessened the proportional effect of the W/L ratio on P_o.

Flat-Bladed Turbines

Experimental data were recorded for flat-bladed turbines having 2,4, 6 and 8 blades, using water, white oil, and a glycerin-water solution in a closed tank, at impeller speeds of 2.58, 4.12 and 6.59 revolutions per second. Removable dividers allowed the tank cross-section to be varied for three conditions: square (impeller centered), rectangular (impeller off-center), and rectangular (impeller centered). The experimental data for lever-arm force and power consumed are listed in Table IV along with certain results calculated from the data. Equations (11) and (13) were used to calculate the Reynolds number, N_{Re}, and the modified power number, P_w.

To correlate the effect of the number of blades, the relationship

$$(P_w)_B = C_B \cdot (P_w)_6 \qquad (16)$$

is used, as discussed in part B. In equation (16) B is the number of blades and C_B is the correlation factor .

As expected, the addition of more blades increased the power consumption for a given system, but with diminishing effect. For water, increasing the blades from 2 to 4 increases the power consumption 60%, while an increase from 4 to 8 blades only increases the power 32%. For the glycerine-water solution power increased 82% for a change from 2 to 4 blades, and

TABLE IV. POWER CONSUMPTION FOR FLAT BLADED TURBINES IN SINGLE-PHASE SYSTEMS

Cross-Section	System	Impeller No.	N Revs/sec.	Force on lever arm, lb.	P Horse-Power	P_w Dimensionless	P_{w/C_6} Dimensionless	N_{Re} Dimensionless
Square	Water	R-0	4.12	0.66	0.05405	5.824	11.83	66,210
			6.59	1.60	0.2093	5.516	11.02	105,900
		R-1	2.58	0.44	0.01391	9.724	12.10	41,460
			4.12	1.01	0.08272	8.912	11.00	66,210
			6.59	2.46	0.3218	8.484	10.39	105,900
		R-2	2.58	0.54	0.01707	12.15	12.15	41,460
			4.12	1.22	0.09992	10.76	10.76	66,210
			6.59	3.02	0.3950	10.42	10.42	105,900
		R-3	2.58	0.54	0.01707	12.15	10.90	41,460
			4.12	1.33	0.1089	11.74	10.70	66,210
			6.59	3.35	0.4382	11.55	10.61	105,900
Square	Glycerine Water	R-0	2.58	0.41	0.01296	7.820	17.86	2,381
			4.12	1.00	0.08190	7.484	16.82	3,802
			6.59	2.33	0.3048	6.812	15.06	6,082
		R-1	2.58	0.69	0.02181	13.16	17.22	2,381
			4.12	1.70	0.1392	12.72	16.51	3,802
			6.59	4.02	0.5258	11.75	15.13	6,082
		R-2	2.58	0.91	0.02876	17.35	17.35	2,381
			4.12	2.23	0.1826	16.69	16.69	3,802
			6.59	5.15	0.6736	15.06	15.06	6,082
		R-3	2.58	1.10	0.03477	20.98	17.98	2,381
			4.12	2.63	0.2154	19.68	17.05	3,802
			6.59	6.11	0.7992	17.86	15.61	6,082
Square	White Oil	R-0	4.12	0.69	0.05651	7.036		295.1
			6.59	1.69	0.2210	6.736		473.2
		R-1	2.58	0.52	0.01644	13.52		185.2
			4.12	1.25	0.1024	12.74		295.1
			6.59	3.25	0.4251	12.95		473.2

TABLE IV. (2)

Cross-Section	System	Impeller No.	N Revs/sec.	Force on lever arm, lb.	P Horse Power	P_w Dimensionless	P_{w/C_6} Dimensionless	N_{Re} Dimensionless
Square	White Oil	R-2	2.58	0.71	0.02244	18.46		185.2
			4.12	1.77	0.1450	18.05		295.1
			6.59	4.72	0.6174	18.81		473.2
		R-3	2.58	0.77	0.02434	20.20		185.2
			4.12	2.15	0.1761	21.92		295.1
			6.59	5.94	0.7770	23.63		473.2
Rectangular off-center	Water	R-0	4.12	0.63	0.05160	5.560	11.30	66,210.
			6.59	1.58	0.2067	5.448	10.89	105,900.
		R-1	2.58	0.42	0.01328	9.452?	11.76	41.460.
			4.12	1.00	0.08190	8.824	10.89	66,210.
			6.59	2.58	0.3375	8.896	10.89	105,900.
		R-2	2.58	2.981	0.09423	11.92	11.92	41,460.
			4.12	2.846	0.2331	11.38	11.38	66,210.
			6.59	2.793	0.3653	11.17	11.17	105,900.
		R-3	2.58	3.375	0.1067	13.50	12.20	41,460.
			4.12	3.132	0.2565	12.58	11.46	66,210.
			6.59	3.086	0.4036	12.34	11.34	105,900.
Rectangular off-center	Glycerine water	R-0	2.58	0.44	0.01391	8.392	19.17	2,381.
			4.12	0.97	0.07944	7.260	16.31	3,802.
			6.59	2.28	0.2982	6.664	14.73	6,082.
		R-1	2.58	0.68	0.02149	12.96	16.93	2,381.
			4.12	1.74	0.1425	13.02	16.90	3,802.
			6.59	4.41	0.5768	12.89	16.60	6,082.
		R-2	2.58	0.91	0.02876	17.35	17.35	2,381.
			4.12	2.19	0.1794	16.38	16.38	3,802.
			6.59	5.11	0.6684	14.94	14.94	6,082.
		R-3	2.58	1.05	0.03319	20.02	17.21	2,381.
			4.12	2.50	0.2048	18.70	16.20	3,802.
			6.59	5.88	0.7691	17.19	15.02	6,082.

TABLE IV. (3)

Cross-Section	System	Impeller No.	N Revs/sec.	Force on Lever Arm, lb.	P Horse-Power	P_w Dimen-sionless	P_w/C_6 Dimen-sionless	N_{Re} Dimen-sionless
Rectangular, Off-Center	White Oil	R-0	4.12	0.65	0.05324	6.628		295.1
			6.59	1.70	0.2224	6.776		473.2
		R-1	2.58	0.52	0.01644	13.52		185.2
			4.12	1.27	0.1040	12.95		295.1
			6.59	3.23	0.4225	12.87		473.2
		R-2	2.58	0.74	0.02339	19.24		185.2
			4.12	1.80	0.1474	18.35		295.1
			6.59	4.58	0.5991	18.25		473.2
		R-3	2.58	0.87	0.02750	22.62		185.2
			4.12	2.16	0.1769	22.02		295.1
			6.59	5.71	0.7469	22.75		473.2
Rectangular, Centered	Water	R-0	4.12	0.63	0.05160	5.560	11.30	66,210.
			6.59	1.61	0.2106	5.552	11.09	105,900.
		R-1	2.58	0.46	0.01454	10.35	12.88	41,460.
			4.12	1.08	0.08845	9.528	11.76	66,210.
			6.59	2.76	0.3610	9.516	11.65	105,900.
		R-2	2.58	0.58	0.01833	13.05	13.05	41,460.
			4.12	1.34	0.1097	11.82	11.82	66,210.
			6.59	3.44	0.4500	11.86	11.86	105,900.
		R-3	2.58	0.64	0.02023	14.40	13.02	41,460.
			6.59	3.90	0.5101	13.45	12.36	105,900.
Rectangular, Centered	Glycerine Water	R-0	2.58	0.36	0.01138	6.864	15.68	2,381.
			4.12	0.86	0.07043	6.752	15.17	3,802.
			6.59	2.19	0.2864	6.400	14.14	6,082.
		R-1	2.58	0.68	0.02149	12.97	16.98	2,381.
			4.12	1.66	0.1360	12.42	16.12	3,802.
			6.59	4.00	0.5232	11.69	15.05	6,082.
		R-2	2.58	0.86	0.02718	16.40	16.40	2,381.
			4.12	2.15	0.1761	16.09	16.09	3,802.
			6.59	5.11	0.6684	14.94	14.94	6,082.
		R-3	2.58	1.00	0.03161	19.07	16.39	2.381.
			4.12	2.44	0.1998	18.26	15.82	3,802.
			6.59	5.87	0.7778	17.16	14.99	6,082.

TABLE IV. (4)

Cross-Section	System	Impeller No	N revs/sec	Force on Lever arm, lb.	P Horse-power	P_w Dimen-sionless	P_w/C_6 Dimen-sionless	N_{Re} Dimen-sionless
Rectangular, Centered	White Oil	R-0	4.12	0.66	0.05405	6.728		295.1
			6.59	1.64	0.2145	6.536		473.2
		R-1	2.58	0.49	0.01549	12.74		185.2
			4.12	1.19	0.09746	12.13		295.1
			6.59	3.08	0.4029	12.27		473.2
		R-2	2.58	0.71	0.02244	18.46		185.2
			4.12	1.78	0.1458	18.15		295.1
			6.59	4.34	0.5677	17.30		473.2
		R-3	2.58	0.83	0.02624	21.58		185.2
			4.12	2.10	0.1720	21.41		295.1
			6.59	5.48	0.7168	21.84		473.2

47% for 4 to 8 blades.

2. Two-Phase Data

Flat paddle A-4 was used for the two-phase mixing studies, with speeds of 4.12 and 6.59 revs/sec for water-air mixtures, and 6.59 revs/sec for white oil-air mixtures. Table V and VI present the data for these two mixtures along with calculations made from the data. The force on the lever arm and the resultant power consumed are shown with the correlation values of modified power number, equation (13), and the reduced power number, P_W/P_W^*, where P_W^* is the value for single-phase (100% liquid) mixing.

The horsepower requirements decrease as more liquid is replaced by air in the closed vessel with a corresponding drop in modified power number, P_W, and the reduced power number, P_W/P_W^*. The largest drop in power requirements is for the condition where the flow pattern resembles a baffled cylindrical tank in the turbulent regime, the rectangular cross-section with impeller centered for the water-air mixtures.

TABLE V. POWER CONSUMPTION FOR WATER-AIR MIXING USING FLAT BLADED PADDLE A-4

Cross-Section	N revs/sec	Volume % water	Force on lever arm, lb.	Power H.P.	P_w Dimensionless	$\frac{P_w}{P_w^*(100\% \text{ liquid})}$
Square	4.12	100	3.74	0.3063	(7.900)**	1.000
		97.5	3.82	0.3128	7.827	0.991
		95	3.71	0.3038	7.602	0.962
		92.5	3.28	0.2686	6.721	0.851
		90	2.76	0.2260	5.655	0.716
Square	6.59	100	9.48	1.240	7.585	1.000
		97.5	9.42	1.232	7.544	0.994
		95	8.09	1.058	6.478	0.853
		92.5	6.35	0.8306	5.085	0.670
		90	5.68	0.7429	4.548	0.599
		85	4.97	0.6501	3.980	0.524
Rectangular, Off-Center	4.12	100	4.12	0.3374	8.433	1.000
		97.5	3.97	0.3251	8.134	0.964
		95	4.84	0.3964	9.917	1.175
		92.5	2.95	0.2416	6.045	0.716
		90	2.69	0.2203	5.512	0.653
		85	2.74	0.2244	5.614	0.665

** Extrapolated value

TABLE V. (2)

Cross-Section	N revs/sec	Volume % water	Force on lever arm, lb.	Power H.P.	P_w Dimensionless	$\frac{P_w}{P_w^*(100\% \text{ liquid})}$
Rectangular, Off-Center	6.59	100	10.32	1.350	8.257	1.000
		97.5	9.74	1.274	7.800	0.944
		95	11.43	1.495	9.153	1.108
		92.5	6.42	0.8397	5.141	0.622
		90	6.20	0.8110	4.965	0.601
		85	5.12	0.6697	4.100	0.496
Rectangular, Centered	4.12	100	7.04	0.5766	14.41	1.000
		97.5	6.65	0.5446	13.62	0.945
		95	6.35	0.5201	13.04	0.902
		92.5	5.00	0.4095	10.24	0.710
		90	3.81	0.3120	7.80	0.541
		85	3.15	0.2580	6.454	0.447
Rectangular, Centered	6.59	100	17.45	2.284	13.96	1.000
		97.5	16.73	2.188	13.40	0.959
		95	14.05	1.838	11.25	0.805
		92.5	10.65	1.393	8.528	0.610
		90	8.84	1.156	7.079	0.506
		85	6.84	0.8947	5.477	0.392

TABLE VI. POWER CONSUMPTION FOR WHITE OIL-AIR MIXING USING FLAT BLADED PADDLE A-4 AT 6.59 REVS/SEC

Geometry	Volume % white oil	Force on lever arm, lb.	Power, H.P.	P_w Dimensionless	$\frac{P_w}{P_w^*}$ (100% liquid)
Square	100	14.18	1.855	13.12	1.000
	97.5	12.70	1.661	11.75	0.896
	95	9.21	1.205	8.523	0.650
	92.5	8.19	1.071	7.579	0.578
	90	7.74	1.012	7.162	0.546
	85	7.14	0.9339	6.607	0.504
Rectangular, Off-Center	100	14.75	1.929	13.65	1.000
	97.5	12.74	1.666	11.79	0.864
	95	9.63	1.260	8.912	0.653
	92.5	8.44	1.104	7.810	0.572
	90	8.04	1.052	7.440	0.545
	85	7.42	0.9705	6.866	0.503
Rectangular, Centered	100	14.91	1.950	13.80	1.000
	97.5	12.87	1.672	11.91	0.863
	95	9.50	1.243	8.791	0.637
	92.5	8.39	1.097	7.764	0.563
	90	7.96	1.041	7.366	0.534
	85	7.52	0.9836	6.959	0.504

B. DISCUSSION

1. Single-Phase Data

The Froude number will have no effect in single-phase power correlations of this study, because the closed liquid-phase system contains no phase boundary. Gravitational forces, therefore, have no chance to influence the surface level or shape of the agitated fluid.

Four-Bladed Flat Paddles

The effect of blade width upon power number has been reported by numerous investigators, the results of several are listed here. O'Connell and Mack (01) found that for the relation $P_o = K(W/L)^g$ the constant K and exponent g varied with the number of blades. For a four-bladed paddle K was 19.4 and g was 1.15. However, Rea and Vermeulen (R1) found the exponent g to be 1.0 for four-bladed paddles in both baffled and unbaffled conditions. From the theoretical relationships in equations (2) and (4), the power, and hence the power number, is directly affected by the blade width.

Table VII shows the values of the exponent g determined from the experimental data of this study. Figure 7 presents these data graphically, and as expected the effect of the blade width varies with N_{Re} in the transition region as well as with vessel geometry. Later on in this section it is determined that the flow-pattern for the rectangular cross-section with impeller centered (curve 1 in Figure 7) largely eliminates swirl and resembles a fully baffled cylindrical tank, and the flow pattern for the square (curve 3) and rectangular with impeller off-center (curve 2) cross-sections involve swirl and more closely resemble an unbaffled cyclindrical tank. For the latter two cross-sections (curves 2 and 3), the value of g approaches a constant

TABLE VII. VALUES OF EXPONENT g FOR THE RELATIONSHIP $P_o \propto (W/L)^g$

N_{Re} Dimensionless	Tank Geometry		
	Square (no dividers)	Rectangular Impeller off - Center (1 divider)	Rectangular Impeller centered (2 dividers)
470	1.091 ± 0.056	1.052 ± 0.039	1.017 ± 0.024
6,000	0.813 ± 0.053	0.840 ± 0.032	0.937 ± 0.082
110,000	0.706 ± 0.02	0.811 ± 0.01	1.167 ± 0.082

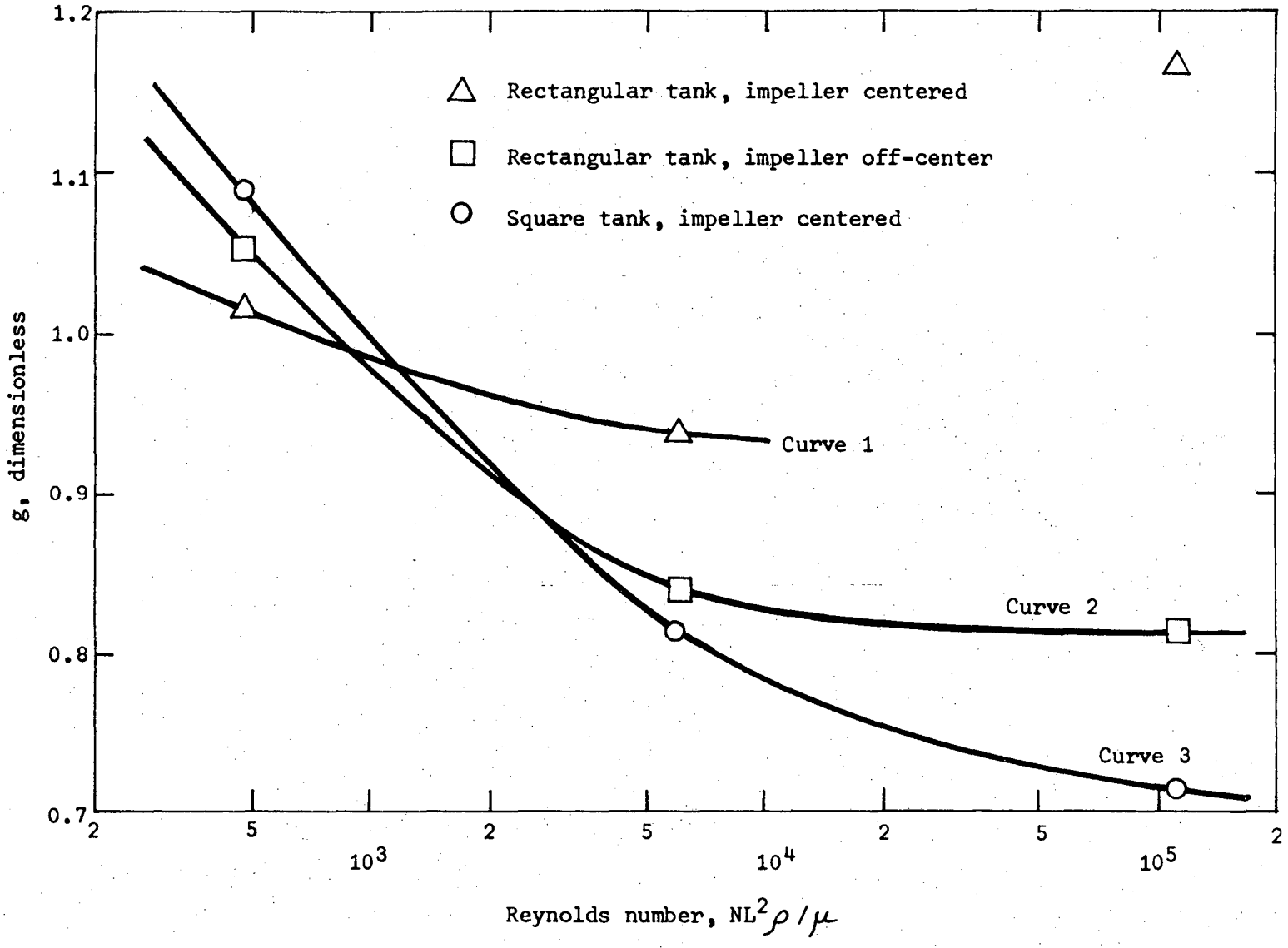

Fig. 7. Values for the exponent g for the relationship $P_o = K(W/L)^g$

XBL 6810-6095

value independent of N_{Re} in the turbulent region. Although all three curves pass through a point where the value of g in $(W/L)^g$ is 1.0, in the transition and turbulent region the more nearly baffled the system the closer the curve remains to a value of g = 1.0.

Even though the data point (on curve 1 of Figure 7) for which the mixing system was in the fully baffled turbulent regime has a value of 1.167, the power consumption, and hence P_o, for paddles A-2 and A-3 in the same system has been shown in part A. of this section to be dependent upon the first power of blade width.

The expression $(W/L)^g$ is for the general condition in which both impeller width W and diameter L vary. Equation (14) is a special case of comparing $(W/L)^g$ for two paddles that have equal diameters, but unequal widths. Therefore, the resultant exponent x for $(W_{A-5}/W_{A-2})^x$ has the same meaning as the exponent g in the general expression $(W/L)^g$.

As already stated, two paddles of equal width, A-2 and A-3, were used for the cross-sections that behaved similar to unbaffled tanks, to explore the effect of impeller diameter L on power consumption. When values of P_o for paddles A-2 and A-3 are compared for systems with the same physical conditions (including rotational speed), the only variables on the right side of equation (10) are the power consumed P and the impeller diameter L. For an impeller P_o decreases gradually but uniformly for unbaffled vessels with increasing N_{Re}. Throughout, at equal speeds, paddle A-3 will have a value of N_{Re} 2.25 times greater than A-2. Thus, when comparing data for paddles A-2 and A-3 to determine the exponent y in equation (15). the calculated values of y would be expected to be lower than the exact dependency because these unbaffled systems have a small dependency upon the

Reynolds number. In view of this, it is not unreasonable to consider the calculated value of y = 3.78 to be within the experimental accuracy of y = 4.0, indicating P_o to be dependent upon L^4.

Although $(L/W)^{1.0}$ cannot be shown to be an exact correlation, it is a good general approximation for the data of this study, agreeing with other investigators and with the theoretical expectations. Equation (13), uses the $(L/W)^{1.0}$ ratio to define the modified power number, P_W,

$$P_W = P_o(L/W)^{1.0} = Pg_c/(\rho N^3 L^4 W) \qquad (13)$$

which is also tabulated in Table II for the flat-bladed paddles.

When the effect of the Froude number is negligible, as it is with closed vessels, impeller power data are presented similarly to Figure 8 which shows the modified power number as a function of Reynolds number. The reference curves 4 and 5 in Figure 8 were taken from the data of Rushton, Costich, and Everett (R2) for a circular cross-section with two-bladed flat paddles adjusted for the paddle width-to-diameter ratio and for the number of blades; curve 4 is for four vertical baffles, each 0.1 of the tank diameter; curve 5 is for an unbaffled vessel. The three experimental curves of this study, curves 1,2, and 3, and the reference curves converge at low Reynolds numbers, in the viscous or laminar flow region, confirming earlier observations that baffling has no effect in the laminar region. In the transition and turbulent regions the data for the three cross-sections of this study, curves 1,2, and 3, fall between the unbaffled and fully baffled conditions of the reference curves depending upon the baffling effect of the particular cross-section.

The term "fully baffled" refers to a flow pattern in which the swirl of the unbaffled vessel is almost eliminated, normally accomplished by placing

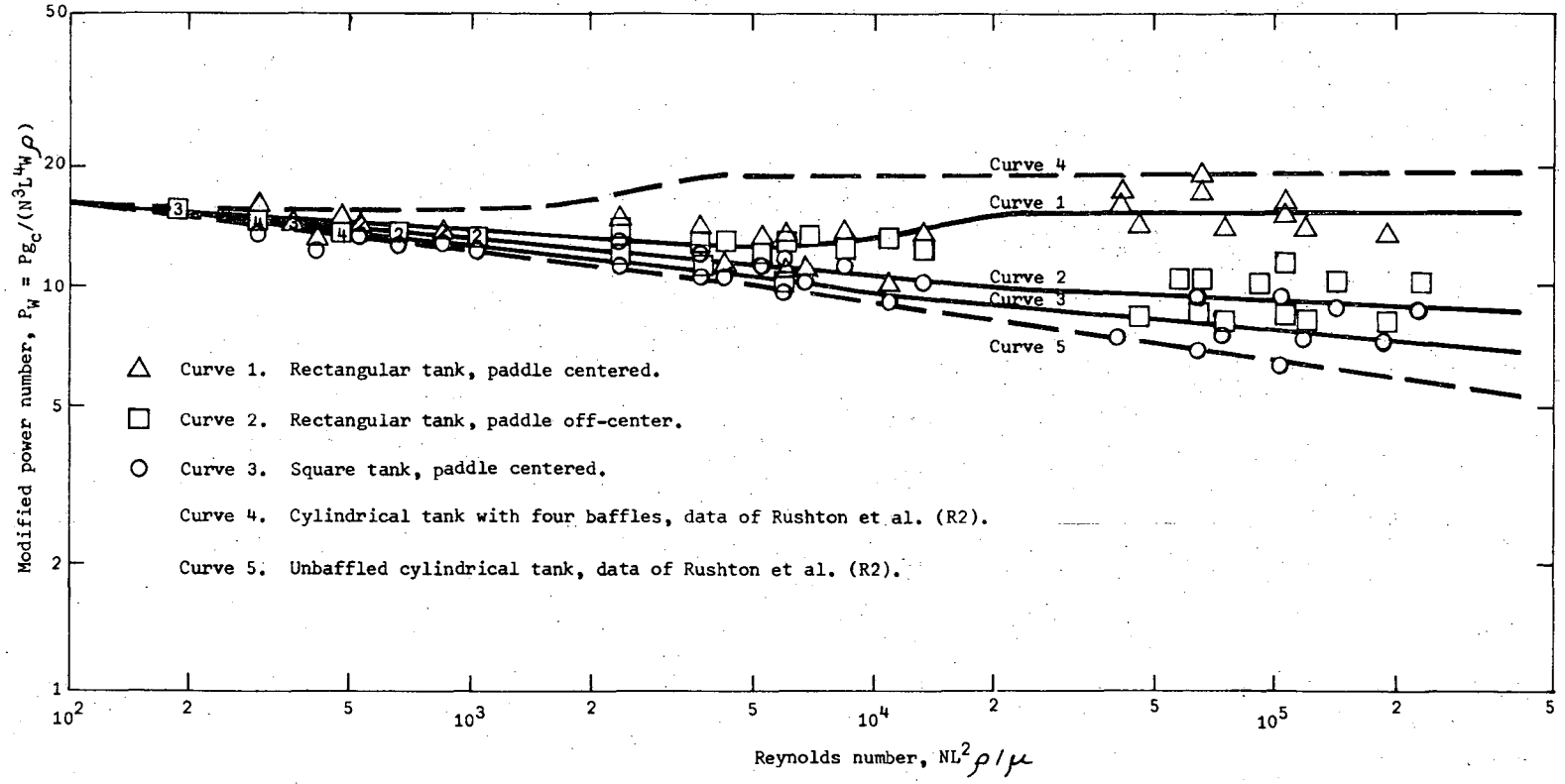

Fig. 8. Modified power number vs. Reynolds number for flat paddles in different tank geometries.

XBL 6810-6096

four or more evenly spaced baffles perpendicular to the vessel wall. The high radial and axial velocities produce several partially independent flow patterns which eliminate the depression around the impeller shaft and flatten out the surface level of open vessels. In a cylindrical tank where four evenly spaced baffles create a fully baffled condition, there would be four similar and symmetrical flow patterns. The change of flow direction of the jet leaving the impeller from radial to axial consumes more power by providing more momentum transfer. For a given impeller and tank geometry, increasing the size and number of baffles will increase the power input to a maximum value beyond which a still larger number of baffles will cause the power consumption to decrease by impeding the axial flow.

Flow patterns and velocity components were not observed in this study, but can be postulated to resemble the ones found in the experimental studies of Nagata et al. (N1,N2,N3) using unbaffled and fully baffled cylindrical tanks. A brief account of their findings is included in Section II.

Experimental curves 2 and 3 in Figure 8 have power numbers which continue to decrease with increasing Reynolds numbers in the same manner as an unbaffled cylindrical tank. However, in the turbulent region, the negative slope is not as great and the values of power number are greater than that of an unbaffled tank. Curve 3, paddle centered in a square cross-section, behaves more like the unbaffled conditions than does curve 2, paddle off-centered in a rectangular cross-section. The lack of baffling allows the liquid to have high tangential velocities and swirl around the impeller shaft.

The square cross-section has some balling effect because the midpoint of the walls are closer to the rotating impeller tip than the corners. The

smoothed wall does not have the same effect as a baffle in a cylindrical tank which protrudes perpendicularly away from the wall, and largely or completely eliminates the swirl. Eddying in the corners of the square vessel does, to some degree, impede the tangential swirl , allowing a greater power input than for an unbaffled tank.

Off-center mounting has often been used to reduce swirl, and can give power consumption nearly equal to that of the fully baffled condition for an optimum agitator location. The rectangular cross-section with impeller off-center, curve 2, creates an unbalanced condition between two opposite walls. The resulting flow pattern appears to retain considerable swirl, but evidence of increased eddying (relative to the square cross-section) is provided by the higher power consumption.

The vessel having rectangular cross-section with the impeller centered, (curve 1), behaves similar to a fully baffled tank, in that the power number eventually rises above its value in the transition region and reaches a constant value in the turbulent region. The lineal distance between the impeller tip and horizontal midpoint of the two parallel dividers ranges from one-fifteenth to one-fourth the impeller length and, in effect, creates two compartments of similar but almost independent flow patterns. This compartmentation introduces large eddy currents, eliminating swirl and increasing the power consumption of this cross-section over the other two in this study. However, the power consumed is still not as great as in a fully baffled cylindrical tank in the turbulent region. The behavior of this cross-section is likely to be more similar to that of a cylindrical tank with two baffles 180° apart, so far unstudied.

Flat-Bladed Turbines

Figure 9 shows a log-log plot of modified power number against Reynolds number for the flat-bladed turbine data, as listed in Table IV. For a given turbine, power consumption is nearly identical for all three cross-sections, indicating the flow patterns to be similar. The curve in Figure 9 for the four-bladed turbine R-1 has power number values that are close to those of curve 2 in Figure 8 for a four-bladed paddle in the rectangular cross-section with impeller off-center. In the rectangular cross-section with impeller centered, the flat-bladed turbines establish a flow pattern containing swirl that has the characteristics of a partially baffled cylindrical tank. Evidently the turbines do not produce the two geometrically similar flow patterns in each end of the vessel that are created by the flat paddle and that allow for greater power consumption. In contrast the turbine performs better than the paddle in the square cross-section, and about the same as the paddle in the rectangular cross-section with impeller off-center.

Both paddles A-2 and A-5 have impeller lengths approximately the same as turbine R-1, so the clearance between the impeller tip and the vessel wall is not a factor.

Rushton, Costich, and Everett (R2) plotted log of power at a given speed vs. log of number of blades B, and correlated the effect of the number of blades by two straight lines which intersect near B = 6. They chose the six-bladed turbine as a basis and made the correlation using the ratio B/6 to the 0.8 power for six blades and less, and B/6 to the 0.7 power for eight to twelve blades. Figure 10 shows this correlation for an impeller speed of 6.59 rev/sec, using the log of P_W vs. log of B.

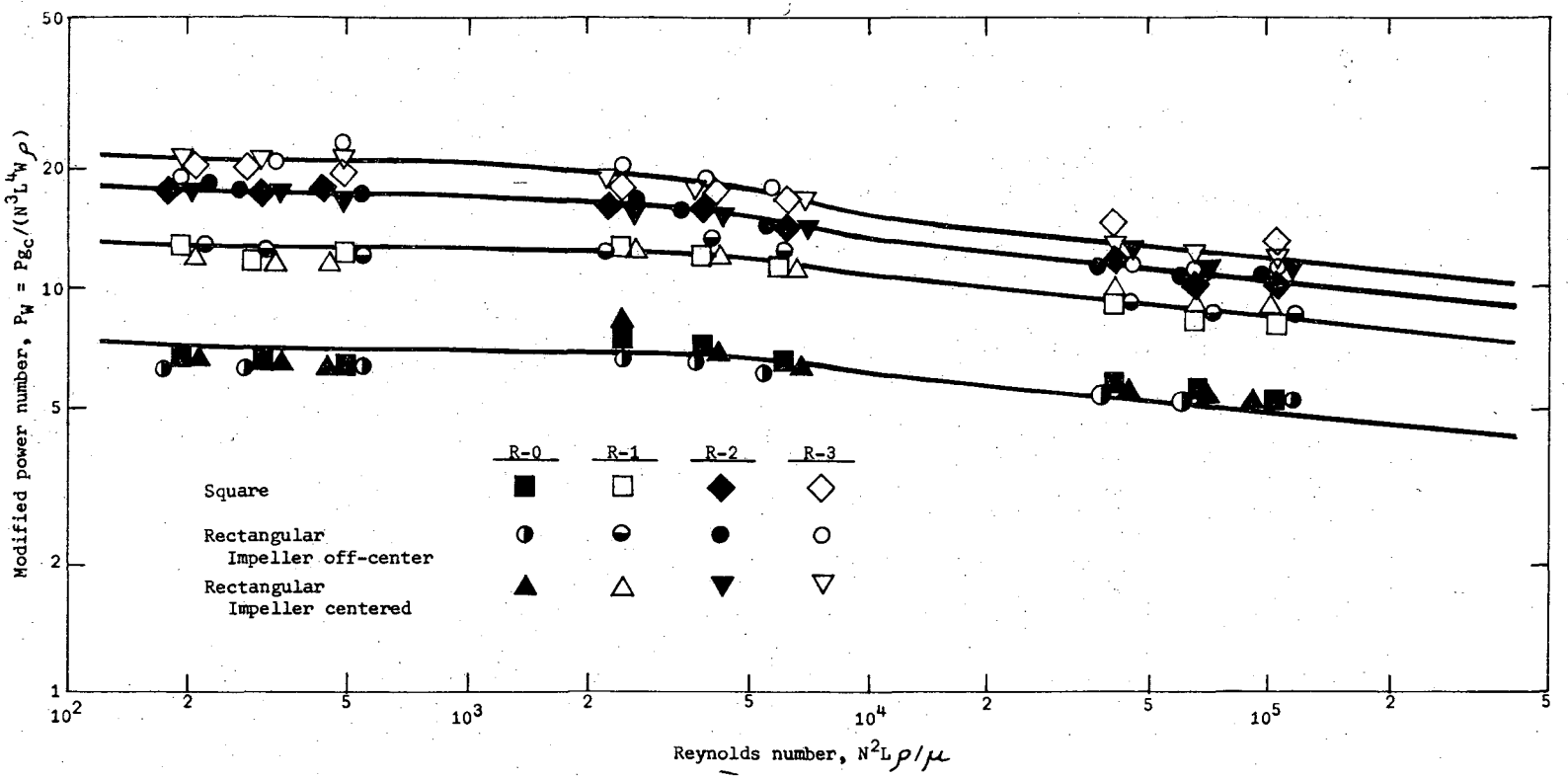

Fig. 9. Power number vs. Reynolds number for flat bladed turbines.

XBL 6810-6097

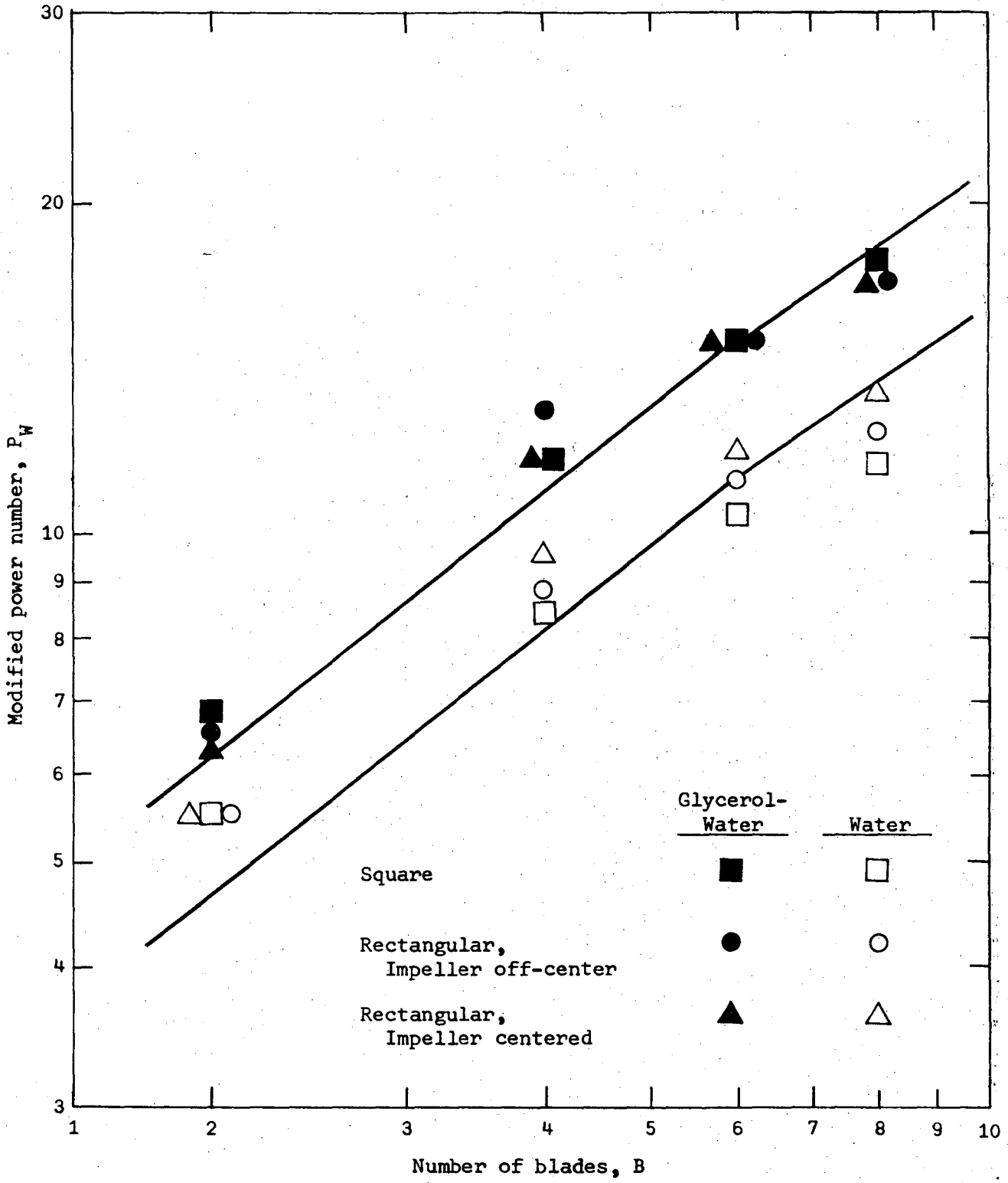

Fig. 10. Power number as a function of the number of turbine blades at 6.59 revs/sec; showing the correlation proposed by Rushton, Costich and Everett(R2).

XBL 6810-6098

A spinning flat-bladed turbine with no blades would merely be a disk which could impart only friction energy to the fluid of a mixing system. As blades are first added, there is a sharp rise in the power input which starts to level off markedly after reaching a certain point. As more blades are added, they are spaced closer together, causing each blade's efficiency to be affected by the blade immediately preceding it. Ultimately so many blades will have been added that the impeller is, in effect, once again a solid piece imparting very little motion or power to the fluid. Somewhere between these two extremes an optimum number of blades B_{opt} occurs, at which point the mixing will achieve the maximum power number $(P_w)_{max}$ for the given system.

This study undertook to improve the correlation of Rushton et al. for the effect of the number of blades upon power input, with the additional goal of finding a correlation which would enable the prediction of blade optimization (maximum power input). To do this, a least-squares computer program was used to test several possible correlating functions against the data. These functions were all selected to give a maximum power number $(P_W)_{max}$ at the optimum number of blades B_{opt}, and to give zero power as B goes to zero. Of the equations tested, the relation

$$P_W = a_3 B e^{-a_4 B} \text{ or } \ln P_W = a_1 + \ln B - a_2 B \qquad (17)$$

gave the best least-squares fit. In this equation P_W is the modified power number, B is the number of blades, and a_1, a_2, a_3, and a_4 are constants at any one Reynolds number. Figures 11, 12, and 13 show the fit of equation 17 to the data. Table VIII lists the original and smoothed values for coefficients a_1 and a_2, and for the smoothed values of $(P_W)_{max}$ and B_{opt}.

To adapt the foregoing solution over a wide range of Reynolds numbers,

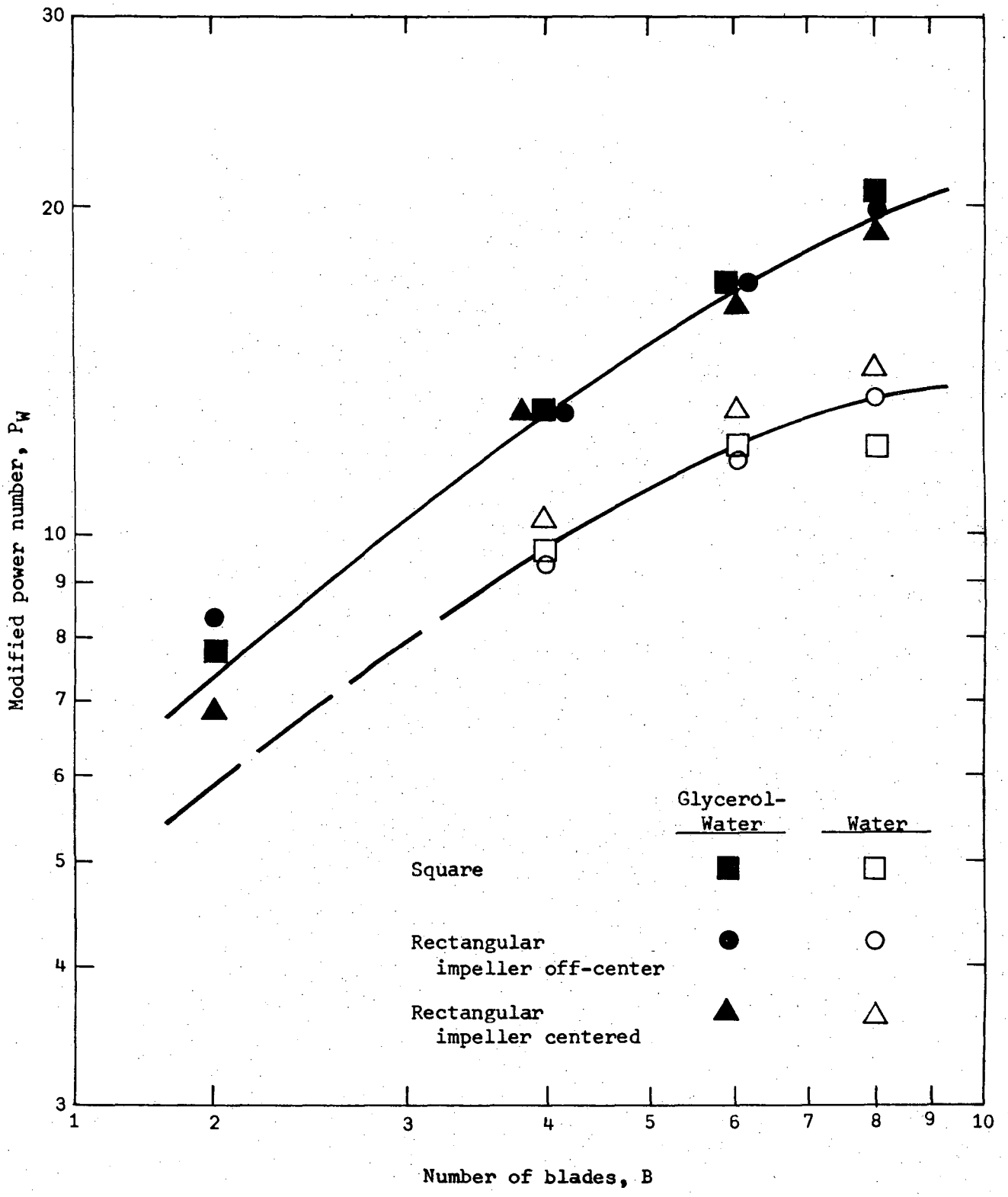

Fig. 11. Individual correlations for the effect of number of turbine blades at 2.58 revs/sec for the relationship $\ln P_W = a_1 + \ln B - a_2 \cdot B$.

XBL 6810-6099

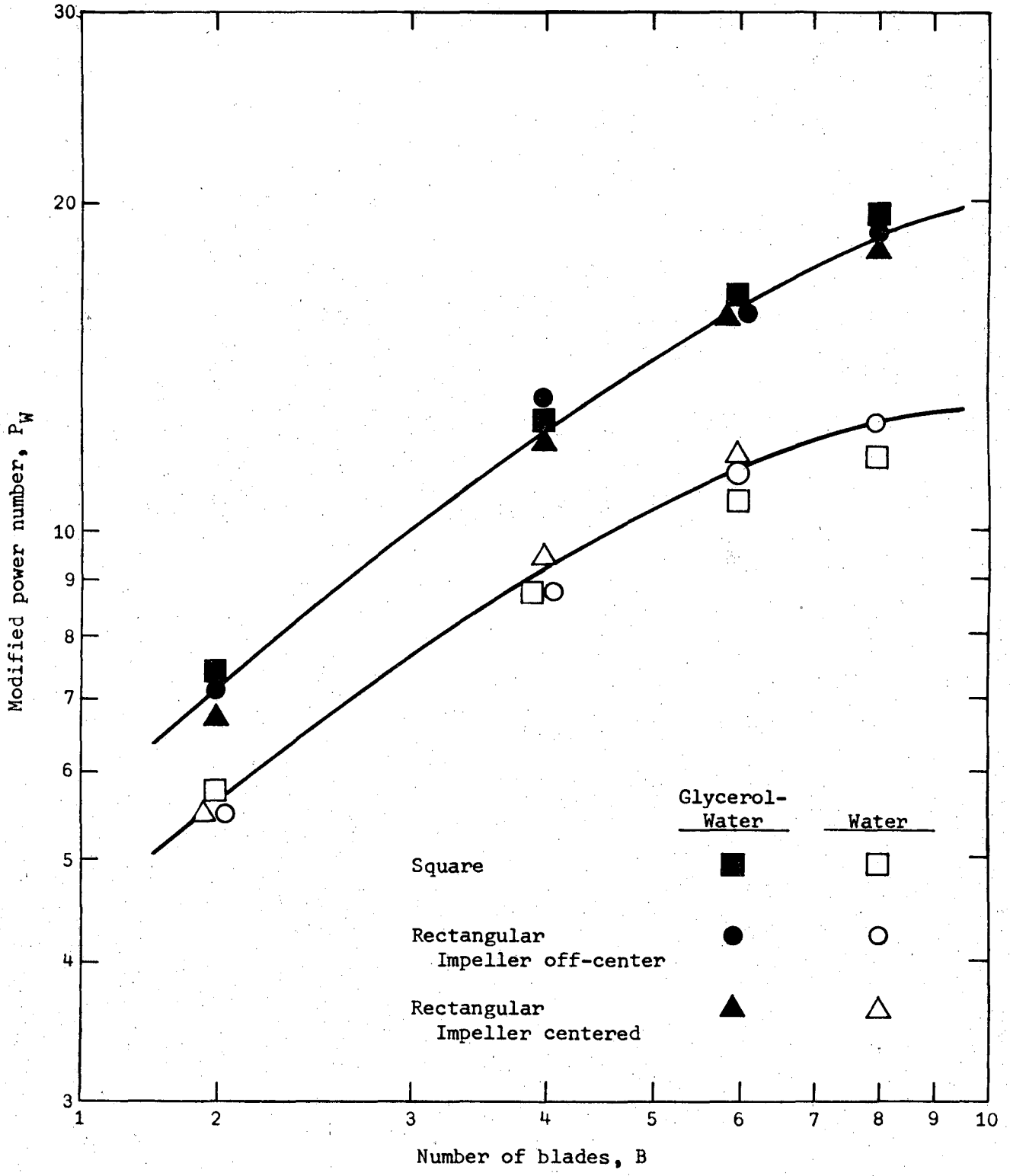

Fig. 12. Individual correlations for the effect of number of turbine blades at 4.12 revs/sec for the relationship $\ln P_W = a_1 + \ln B - a_2 \cdot B$.

XBL 6810-6100

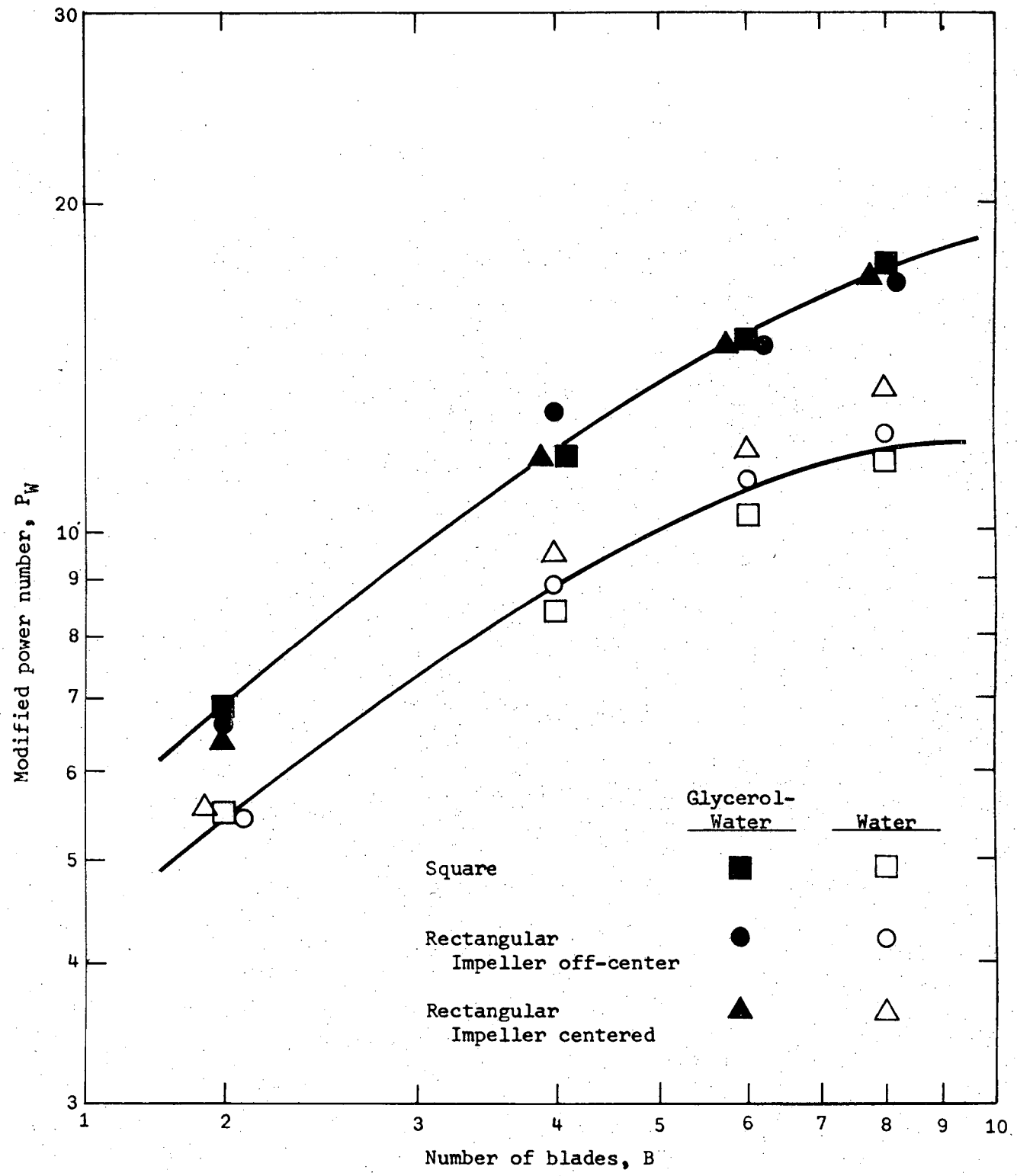

Fig. 13. Individual correlations for the effect of number of turbine blades at 6.59 revs/sec for the relationship $\ln P_W = a_1 + \ln B - a_2 \cdot B$.

XBL 6810-6101

Table VIII. Solutions for the relationship $\ln P_w = a_1 + \ln B - a_2 \cdot B$ for flat bladed turbines

System	N, revs/sec	Coefficients from Computer solution a_1	Coefficients from Computer solution a_2	values obtained from smoothing computer solution a_1	values obtained from smoothing computer solution a_2	values obtained from smoothing computer solution B_{opt}	values obtained from smoothing computer solution $(P_w)_{max}$
Glycerol-Water	2.58	1.476	0.07107	1.456	0.06812	14.57	23.01
	4.12	1.424	0.07016	1.426	0.07224	13.87	21.25
	6.59	1.362	0.07264	1.395	0.07639	13.20	19.61
Water	2.58	1.297	0.09784	1.269	0.09331	10.80	14.13
	4.12	1.238	0.10210	12.38	0.09744	10.28	13.05
	6.59	1.195	0.09526	1.207	0.10158	9.786	12.04

the parametric values determined by equation 17 were plotted against Reynolds number as in Figures 14 and 15. For another system with dynamic and kinematic similarity as discussed in the introduction of this section, a designer could use Figures 14 and 15 to choose the optimum number of blades for a flat-bladed turbine of like design.

Because the flat-bladed turbines in use today often have six blades, the six-bladed turbine in this study was used as the reference value for correlating the effect of the number of blades upon modified power number:

$$(P_W)_B = C_B \cdot (P_W)_6 \qquad (16)$$

Values for the ratio C_B as determined from the data, are shown on Figure 16 as a function of Reynolds number. The interpolated values for the twelve bladed turbine decrease more rapidly than values for the eight bladed turbine because at N_{Re} above 15,000 the optimum number of blades is below twelve and decreasing steadily. This puts the twelve bladed turbine on the down side of the P_o vs. B curve above N_{Re} of 15,000 instead of on the upside like the eight bladed turbine.

For a given impeller in a given system Reynolds number is only a function of the impeller speed. The faster the impeller rotates the quicker the second blade sweeps the area vacated by the first blade. The fluid has more velocity and, hence, more kinetic energy when it comes in contact with the second blade. For this reason the second blade is able to impart less energy, or power, to the fluid and is less efficient than it would be at slower speeds. For the same reason, adding blades has relatively less effect at higher Reynolds numbers. From Figure 14 the optimum number of blades decreases from 15 at N_{Re} = 2000 to 10 at N_{Re} = 100,000. As predicted the values of C_B in Figure 16 move toward 1.0 at higher Reynolds

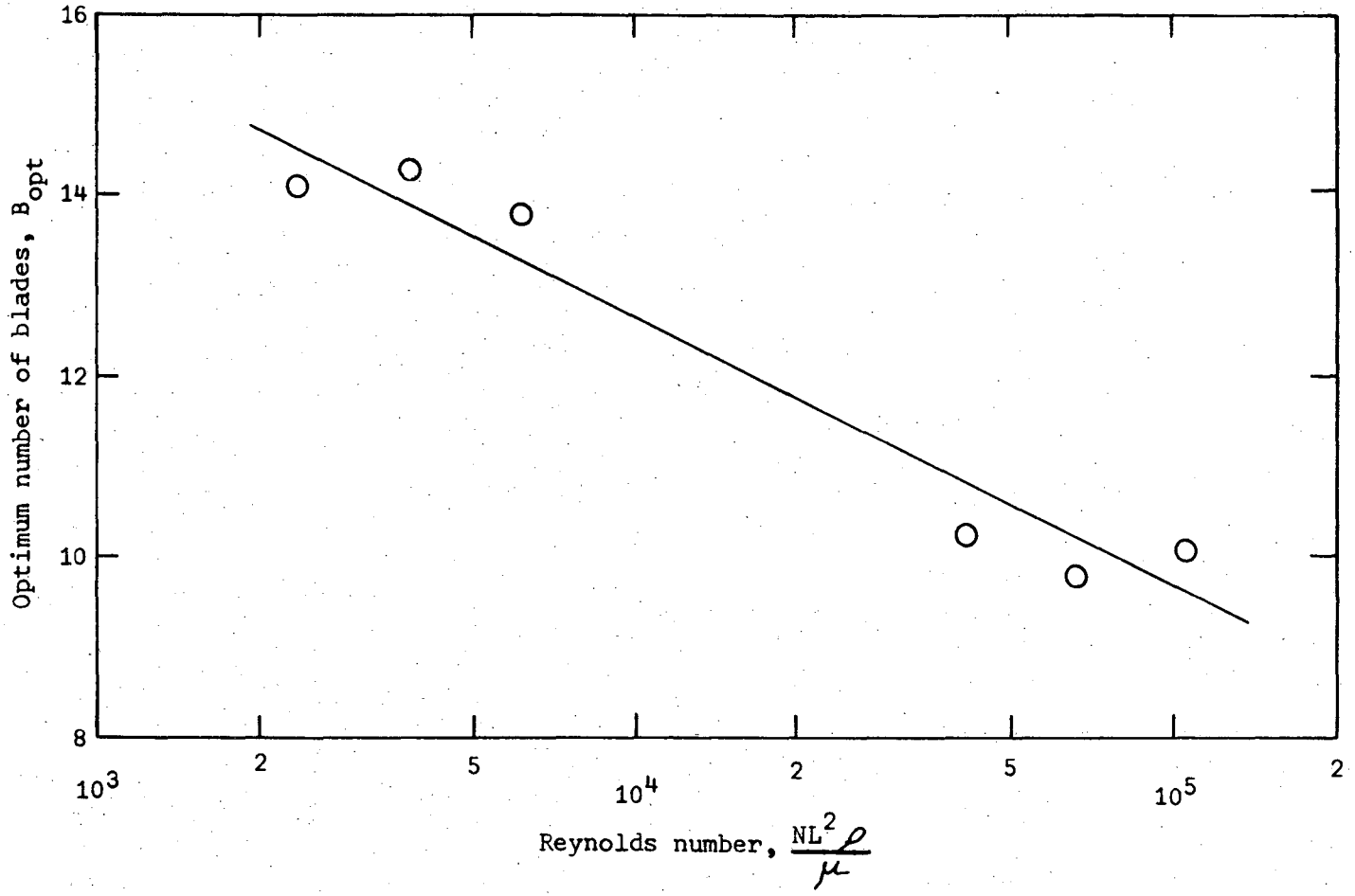

Fig. 14. Determination of the optimum number of turbine blades based on the relationship $\ln P_W = a_1 + \ln B - a_2 \cdot B$.

XBL 6810-6102

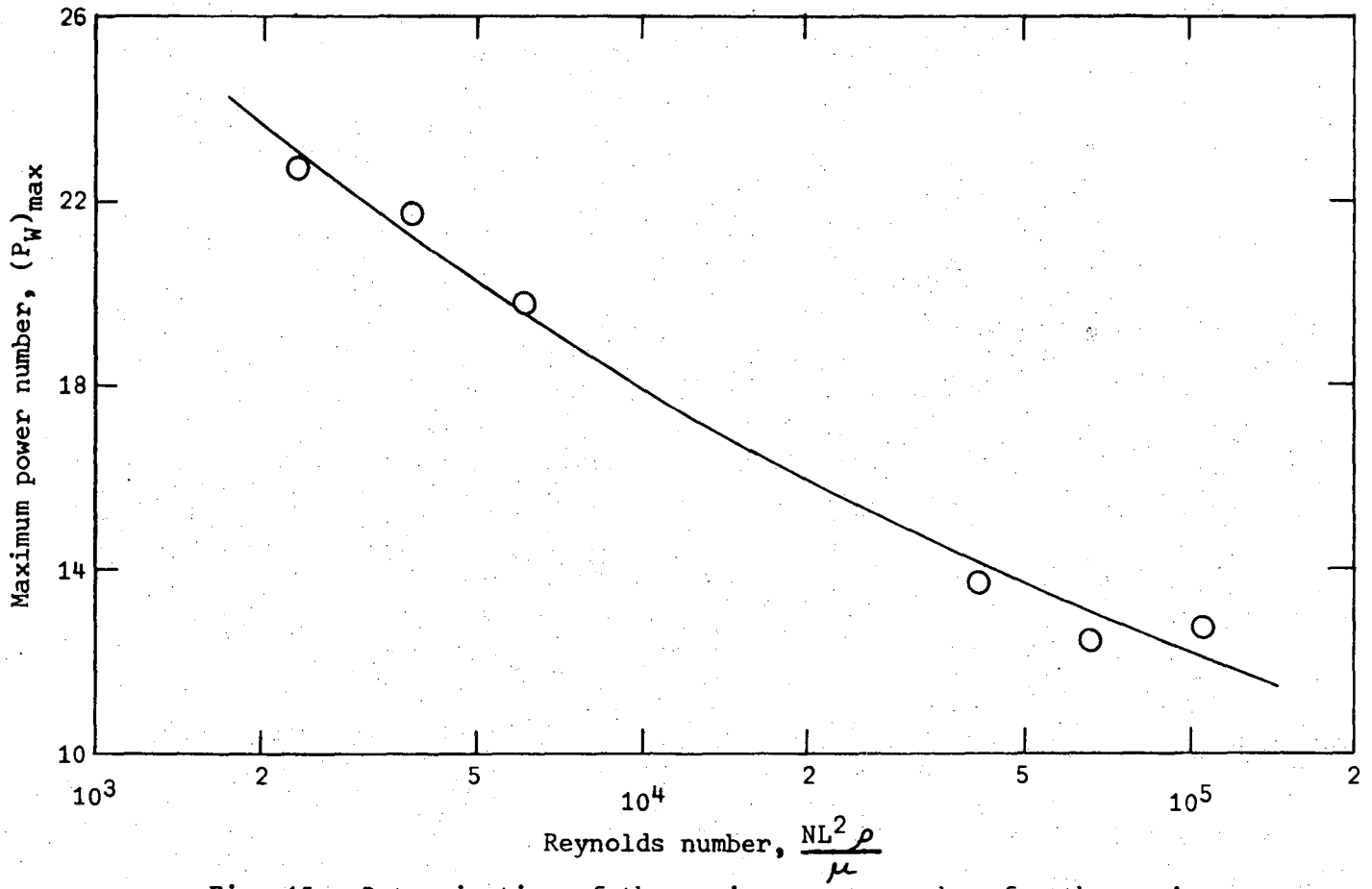

Fig. 15. Determination of the maximum power number for the optimum number of turbine blades for the relationship $\ln P_W = a_1 + \ln B - a_2 \cdot B$.

XBL 6810-6103

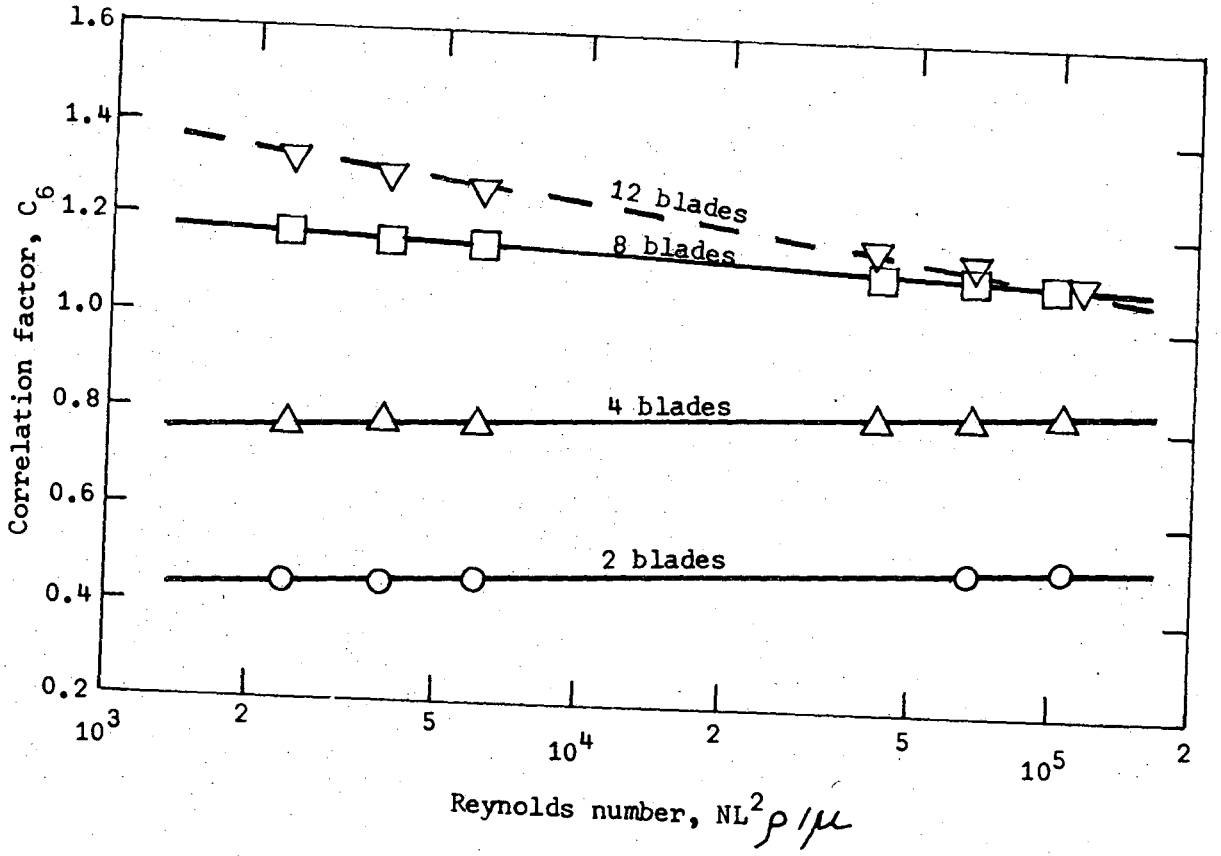

Fig. 16. Six bladed correlating factor for turbines for Reynolds numbers of 1000 to 200,000.

XBL 6810-6104

numbers, possibly indicating a lesser effect of additional blades and the decreased efficiency of all blades when more are added.

Figure 17 presents the correlated data of this study with reference curves from Rushton et al.(R2) for a six-inch diameter turbine with six flat blades in a open circular tank for both baffled and unbaffled conditions. The characteristics of curve 3 are the same as previously discussed for the experimental curves of Figure 9.

If the same mathematical and graphic approach presented in this study to determine the effect of the number of blades was applied to a baffled cylindrical vessel, the general solutions would be similar to the findings of this study although specific values would differ. For example, the values of power number would be higher for the baffled than the unbaffled vessels, and the baffled system would still have an optimum number of blades (maximum power input) which would decrease at higher Reynolds numbers. It is anticipated that the optimum number of blades for baffled cylindrical vessels would also be in the range of 10 to 16. In most instances a designer would choose the most efficient impeller which would have a number of blades equal to or close to the optimum value of 10 to 16. The number of blades for the reference impeller for correlating the effect of the number of blades should also be near the optimum, say eight or twelve, depending upon the results of the fully baffled cylindrical tank study.

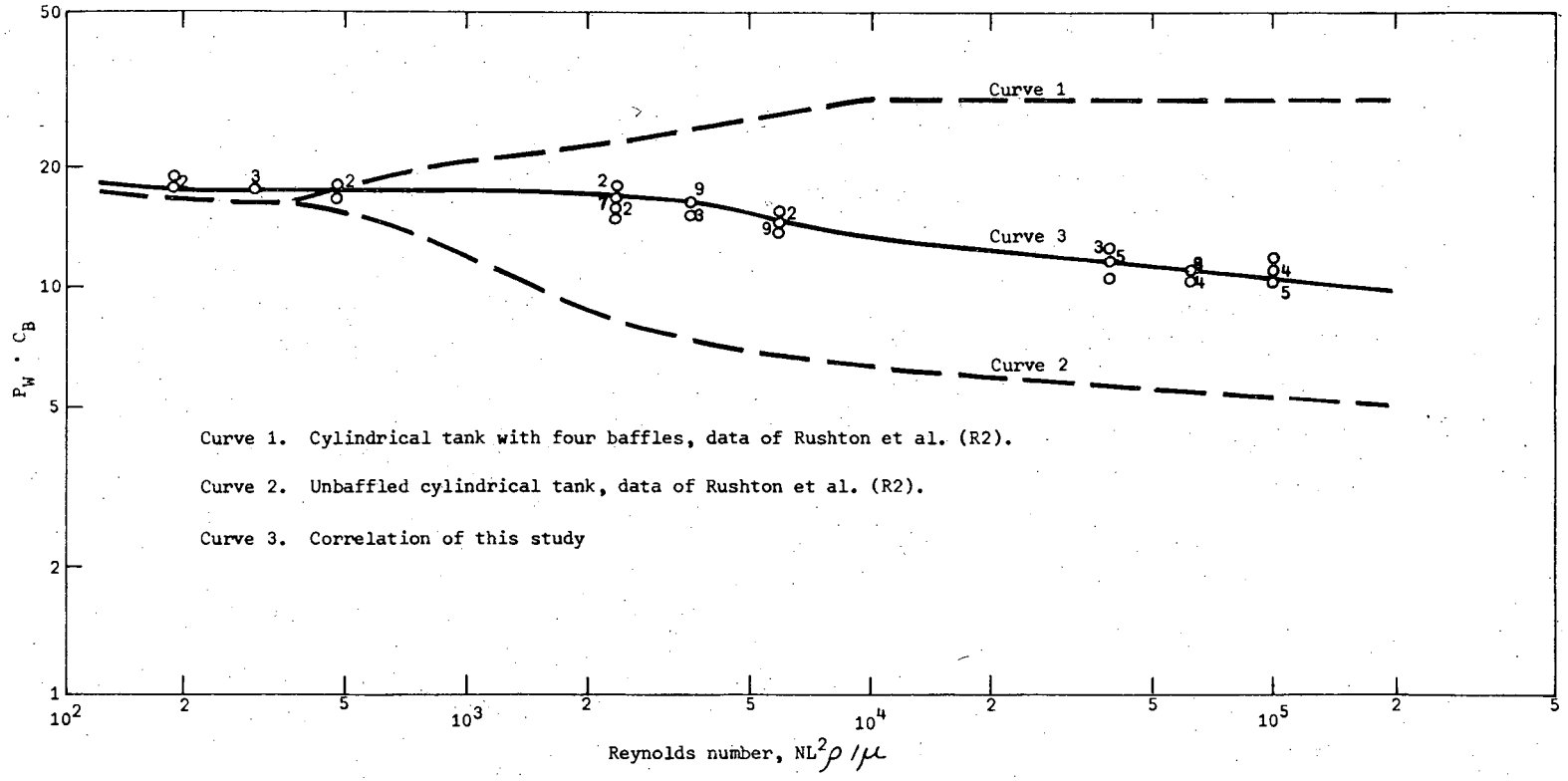

Fig. 17. Correlating turbines to the six bladed turbine for Reynolds numbers of 1000 to 200,000.

XBL 6810-6105

2. Two-Phase Data

When a liquid system is in contact with a gas phase in a closed vessel, the gas phase will tend to be introduced downward into the liquid during agitation, and may cause reduction in the power input (and therefore in the power number).

Rushton, Costich, and Everett (R2) report that any shape of impeller operating on a vertical centerline of a smooth-walled unbaffled cylindrical tank will produce rotary and circular laminar flow, resulting in a swirl, or vortex, with the minimum of vertical flow currents. Taylor and Metzner (T1,M2) found that systems which are baffled at high Reynolds numbers produce flow patterns that exist in which there are regions of high shear where fluids flowing in opposite directions meet. It is always at the upper ridge or seam made by this high-shear region that air is introduced into the liquid, being carried downward into the impeller and causing a decrease in the power number.

Rushton et al.(R2) and Clark and Vermeulen (C1) suggest the use of the Froude number to correlate the power number and surface phenomena of this type, since N^2L/g gives the ratio of inertial to gravitational forces. Clark and Vermeulen found that the impeller depth was important, due to an increase in upper-surface velocity components as the impeller is brought closer to the top of the liquid.

Figure 18 shows the correlation as proposed by Clark and Vermeulen for liquid-air mixing in a baffled cylindrical tank, along with selected data from this study. These data, as shown in Table IX, are for flat paddle A-4 in the rectangular cross-section with paddle centered using speeds of

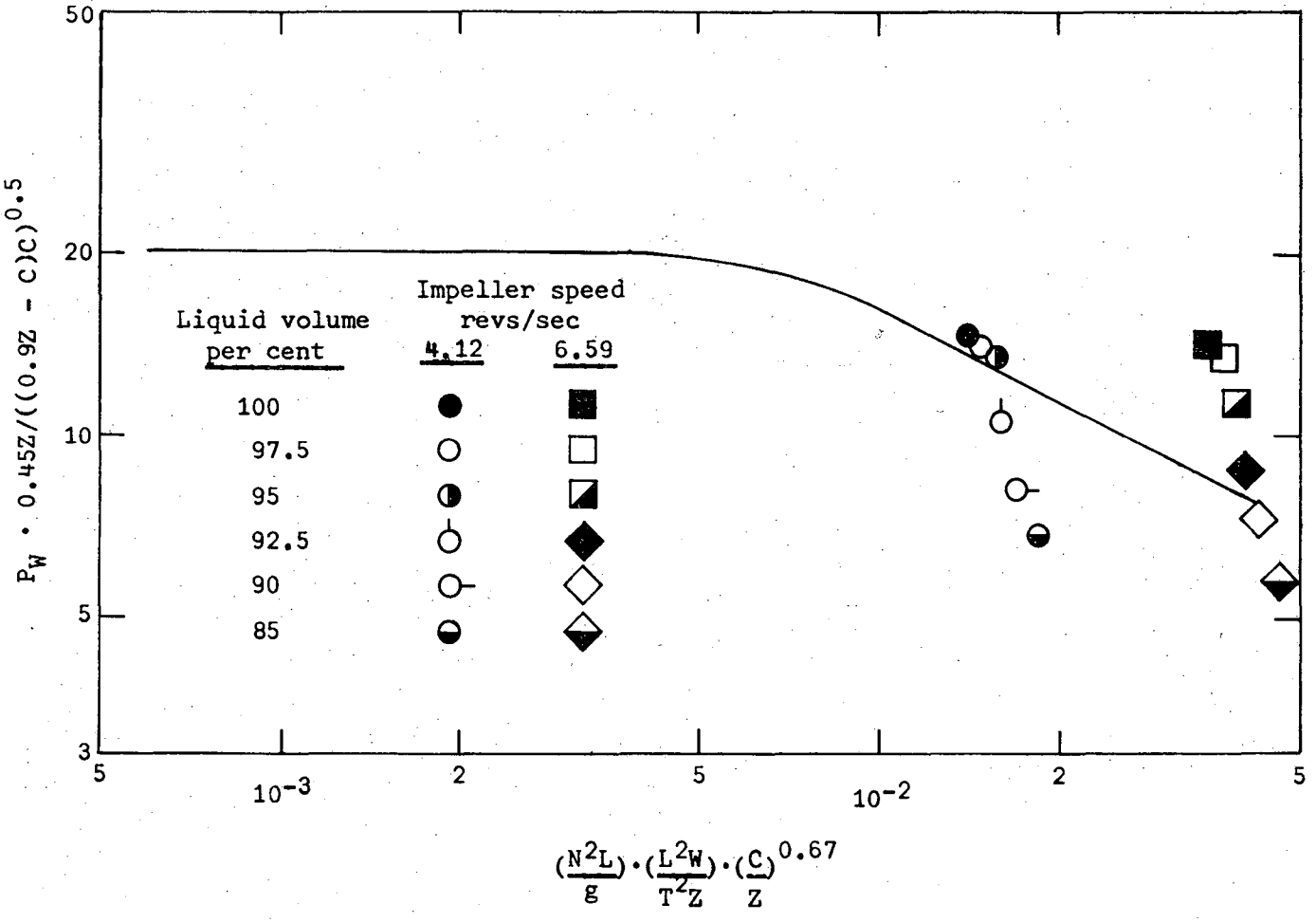

Fig. 18. Comparison of water-air mixing data with the correlation of Clark and Vermeulen

XBL 6810-6106

TABLE IX. EXPERIMENTAL DATA FOR FLAT PADDLE A-4 IN WATER-AIR MIXTURE USING A RECTANGULAR CROSS-SECTION, IMPELLER CENTERED

N revs/sec	Volume % water	$P_w \frac{0.45Z}{[(0.9Z-C)C]^{0.5}}$	$\frac{N^2L}{g} \cdot \frac{L^2W\pi}{4T_1T_2Z} \cdot \left(\frac{C}{Z}\right)^{0.6}$
4.12	100	14.50	0.01427
	97.5	13.76	0.01489
	95	13.22	0.01555
	92.5	10.46	0.01614
	90	8.026	0.01702
	85	6.777	0.01874
6.59	100	14.04	0.03653
	97.5	13.53	0.03809
	95	11.41	0.03978
	92.5	8.707	0.04129
	90	7.284	0.04354
	85	5.719	0.04794

4.12 and 6.59 revs/sec in water-air mixtures. It is necessary to modify the geometrical factor of the abscissa term to account for the rectangular cross-section. This impeller-to-tank-volume ratio then becomes $(\pi L^2 W)/(4 T_1 T_2 H)$, where T_1 and T_2 are the tank cross-section dimensions.

Table V lists the data of this study for the water-air systems while Table VI gives the data for the white oil-air systems. The reduced power number, P_w/P_w^*, is used to present the data graphically in Figures 19, 20, and 21. P_w^* is the power number for 100% liquid mixing for each particular system.

Since the impeller position relative to the vessel was the same for all runs, the more air that was placed in the system, the closer the impeller was to the liquid surface, and the more effect the impeller had on the surface interface. For small amounts of air (up to 3 - 6%) in the turbulent region the gaseous phase is most probably drawn into the liquid by the interaction of the liquid with the vessel cover and dispersed by the bulk flow pattern. The inability of the dispersed air to coalesce and collect at the impeller accounts for the lack of effect that small amounts of induced air have upon the power. For gaseous amounts above 3-6% the reduced power number, P_w/P_w^*, drops off quite rapidly as vortexing begins and larger amounts of air come in contact with the surface of the impeller. After a point the liquid around the impeller becomes somewhat saturated with entrained air and increasing the volume fraction of air does not increase the amount of air entrainment as rapidly. This causes the reduced power number P_w/P_w^*, to decrease at a lower rate.

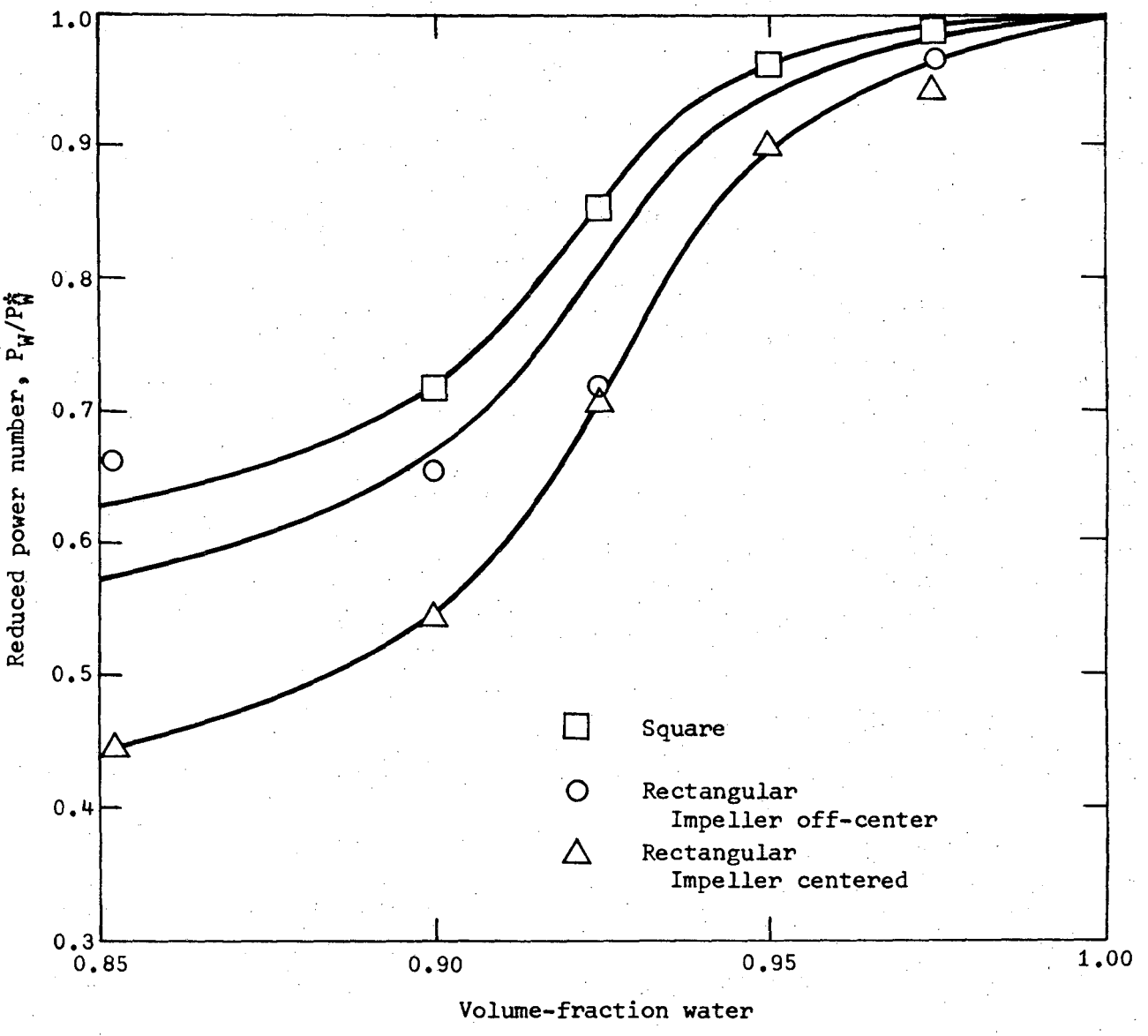

Fig. 19. Reduced power numbers for water and air mixing, using flat bladed paddle A-4 at 4.12 revs/sec.

XBL 6810-6107

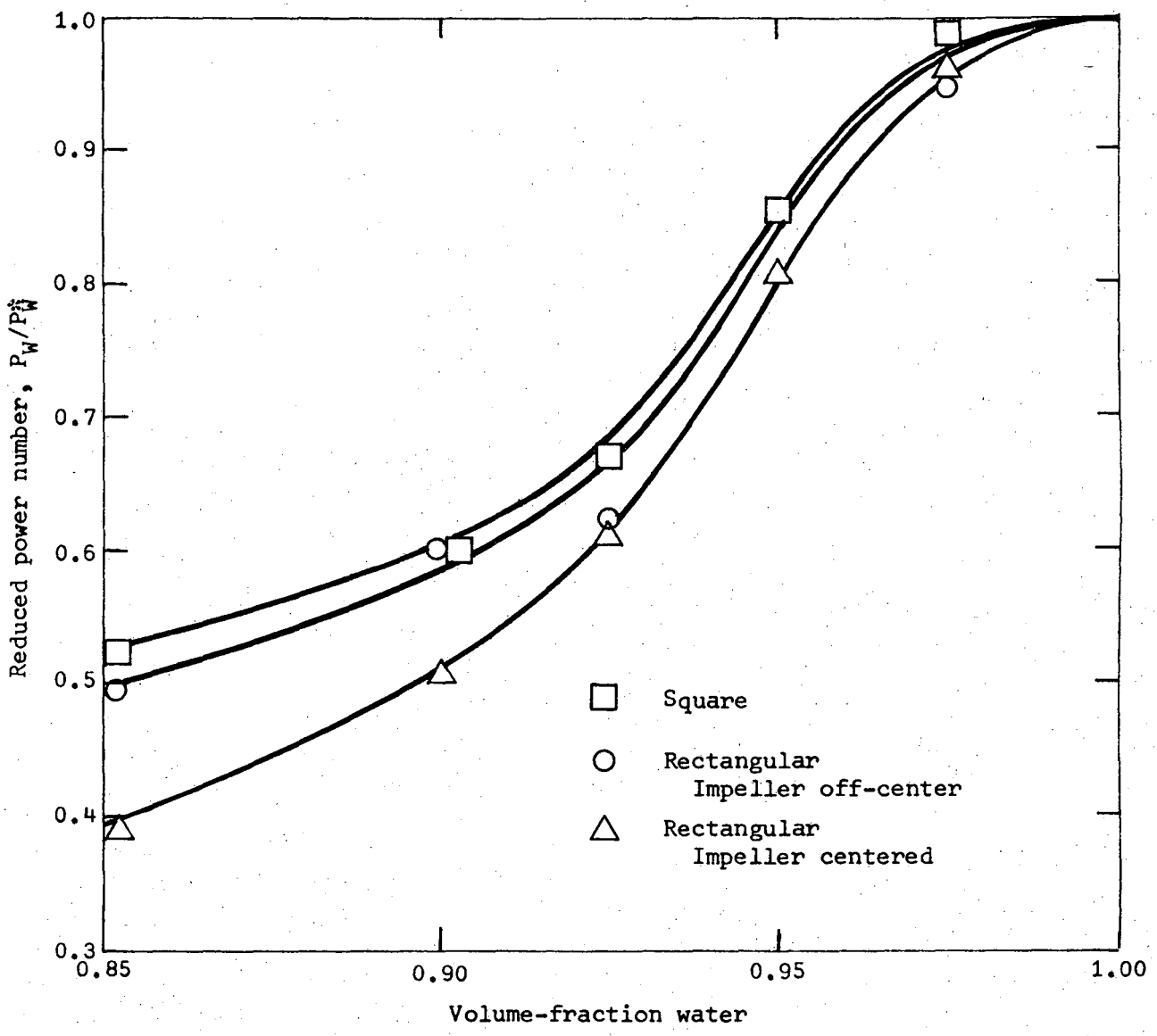

Fig. 20. Reduced power numbers for water and air mixing, using flat bladed paddle A-4 at 6.59 revs/sec.

XBL 6810-6108

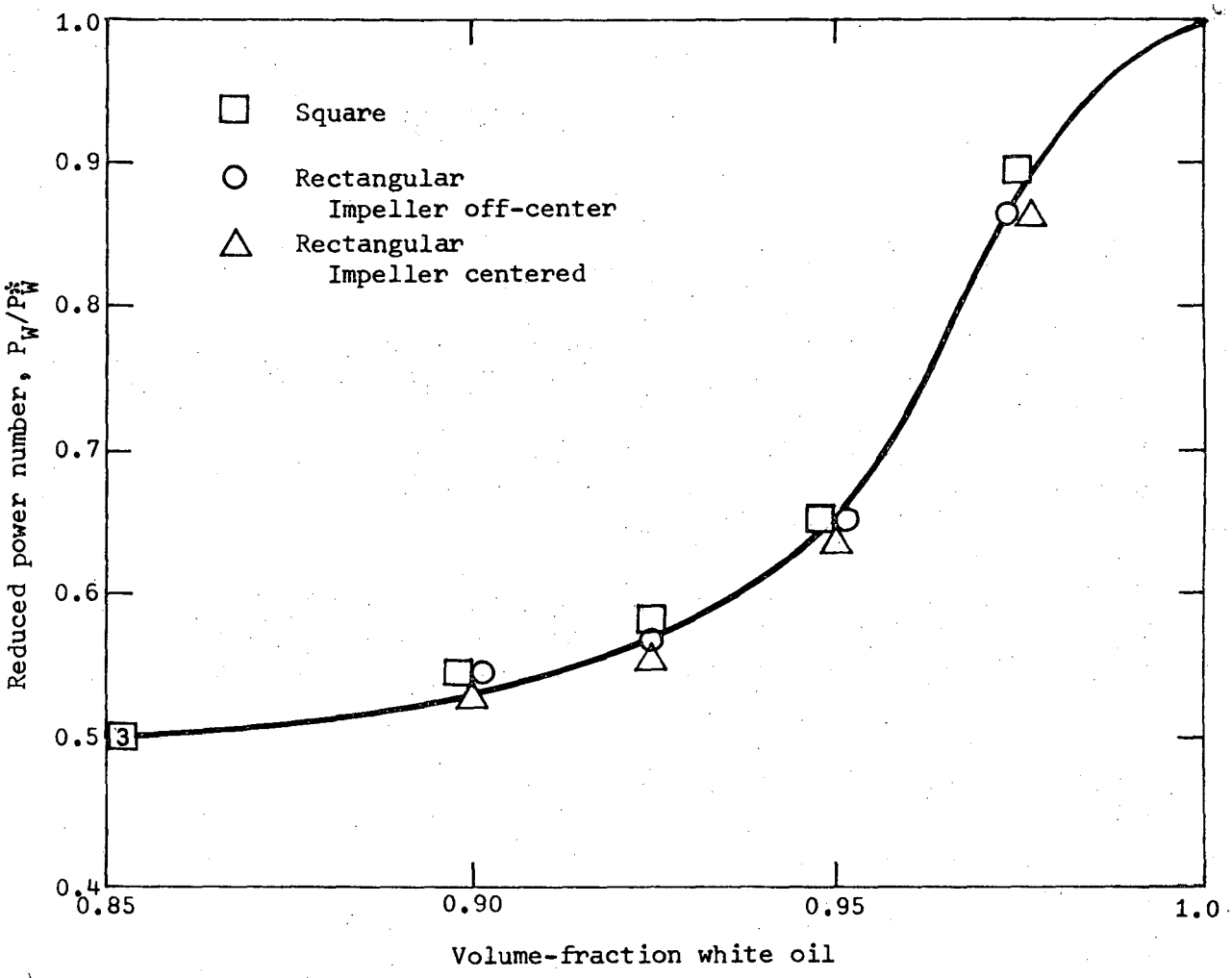

Fig. 21. Reduced power number for white oil and air mixing, using flat bladed paddle A-4 at 6.59 revs/sec.

XBL 6810-6109

For the water-air systems, the cross-section that has the most baffling effect, impeller centered in the rectangular cross-section, has the greatest reduction of reduced power number. The actual values for power number do behave as anticipated; that is, with all other factors equal, the more baffling effect the vessel geometry has, the larger the power number. The square cross-section has the least baffling effect, and by similar reasoning is least effected by the introduction of air into the agitated liquid.

The white oil - air systems are in the lower end of the transition region near the laminar region, where baffling has negligible effect on power input. This is demonstrated in Figure 8 where the power numbers converge at lower Reynolds numbers and by Figure 21 which shows the reduced power numbers for the white oil-air mixtures to be independent of vessel cross-section.

V. CONCLUSIONS

1. Present power correlations for radial-flow impellers use an impeller Reynolds number, $NL^2\rho/\mu$, based only on impeller length (diameter). Consideration should be given to a Reynolds number which includes the total net flow through or area swept by the impeller, having a form such as $NLW\rho/\mu$ or $(NL^2\rho/\mu)(W/T)$ to include the effect of impeller width.

2. Power requirements for liquid agitation in a closed rectangular tank with both four-bladed flat paddles and various flat-blade turbines fall between the fully baffled cylindrical tank and the unbaffled cylindrical tank, the exact location depending upon the specific cross-section and the paddle position. Power requirements for cross-sections studied may be predicted from general correlations presented in Figures 8 and 9.

3. For a flat-bladed turbine, the optimum number of blades, the number which produces maximum power input at any given rotor speed, decreases linearly with respect to the logarithm of the Reynolds number, from a value of 16 at $N_{Re} = 10^3$ to a value of 10 at $N_{Re} = 10^5$. The six-bladed turbine in general use consumes 27.5% less power at $N_{Re} = 10^3$ than a turbine of 12 blades, and 8.3% less power at $N_{Re} = 10^5$. By using a turbine nearer the optimum number of blades, the needed agitation can be achieved at a lower rotational speed, thereby increasing the economic life of the bearing surfaces for both the motor and the drive-shaft. The correlation developed for the effect of the number of blades and for the optimum number of blades for disk turbines should also apply to a cylindrical tank, although there has been no experimental confirmation.

4. For liquid/air mixing, baffled systems consume more power than unbaffled

systems and experience a greater loss in power input in the transition and turbulent regimes. As for single-phase liquid agitation, vessel cross-section has no effect for two-phase mixing in the laminar regime.

NOTATION

a_1, a_2, etc.	coefficients
a, b, c, etc.	exponents
B	number of blades on a flat bladed turbine impeller
B_{opt}	optimum number of blades for a given system
C	distance from center of impeller to tank bottom, ft.
C_B	correlation factor for turbine impellers
d	characteristic length (for instance, L), ft.
g	gravitational acceleration, ft./min.^{2}
g_c	conversion factor between force and mass, lb. ft./(lbf. min.^{2})
H	theoretical impeller head, ft. lbf./lb.
k	ratio of tangential fluid velocity at the periphery of an impeller to the peripheral impeller velocity
K	constant
l	blade length, ft.
L	impeller diameter, ft.
n	number of blades
N	impeller speed, revolutions/sec.
N_{Fr}	Froude number, N^2L/g, dimensionless
N_Q	impeller discharge coefficient, $Q/(NL^3)$, dimensionless
N_{Re}	Reynolds number, $NL^2\rho/\mu$, dimensionless
p	pitch of blades
P	power input to the impeller, ft. lbf./min.
P_o	power number, $Pg_c/(N^3L^5\rho)$, dimensionless
P_w	modified power number, $Pg_c/(N^3L^4W\rho)$, dimensionless
P_w^*	modified power number (100% liquid reference condition)

$(P_w)_{max}$	maximum power number for turbines at B_{opt}
Q	impeller discharge rate, ft.^{3}/min.
r	radial distance from the center of agitator shaft, ft.
T	tank diameter, ft.
T_1, T_2	rectangular tank cross-section dimensions, ft.
v_c	fluid velocity leaving the periphery of an impeller, ft./min.
v_p	peripheral impeller velocity, ft./min.
v_r	radial velocity component, ft./min.
v_w	fluid velocity relative to impeller blade tip, ft./min.
v_z	axial component of fluid velocity, ft./min.
W	impeller width, ft.
x, y	exponents
Z	fluid depth in vessel, ft.
α	angle between velocity vectors, v_c and v_p (see Fig. 1)
β	angle between impeller tip and velocity vector v_p (see Fig. 1)
μ	fluid viscosity, lb./(ft. min.)
ρ	fluid density, lb./ft.^{3}
ω	angular velocity of impeller, radians/min.
ϵ	power input per unit mass, ft.^{2}/min.^{3}
ν	kinematic viscosity of fluid, ft.^{2}/min.

BIBLIOGRAPHY

B1 Bates, R.L., Fondy, P.L., and Fenic, J.G., "Mixing", Vol. 1, ed. by Uhl, V.W., and Gray, J.B., Academic Press, New York and London, 1966

B2 Brodkey, R.S., "Mixing", Vol. 1, ed. by Uhl, V.W., and Gray, J.B., Academic Press, New York and London, 1966

C1 Clark, M.W., and Vermeulen, T., Power Requirements for Mixing of Liquid-Gas Systems (M.S. Thesis), Lawrence Radiation Laboratory Report UCRL - 10996, August 30, 1963 (unpublished)

G1 Gray, J.B., "Mixing", Vol. 1, ed. by Uhl, V.W., and Gray, J.B., Academic Press, New York and London, 1966.

H1 Hinze, J.O., A.I.Ch.E.J 1,289 (1955)

H2 Hixson, A.W., and Baum, S.J., Ind. Eng.Chem., 34, 194 (1942)

M1 Mack, D.E., Chem. Eng.Progress, 47,1099 (1951)

M2 Metzner, A.B., and Taylor, J.S., A.I.Ch.E.J.,6, 109 (1960)

N1 Nagata, S., Yamamoto, K., Hashimoto, K., and Naruse, Y., Mem. Fac. Eng. Kyoto Univ., 21,260 (1959)

N2 Nagata, S., Yamamoto, K., Hashimoto, K., and Naruse, Y., Mem. Fac. Eng. Kyoto Univ., 22,68 (1960)

N3 Nagata, S., Yamamoto, K., and Ujihara, M., Mem. Fac. Eng. Kyoto Univ., 20,336 (1958)

N4 Nagata, S., and Yokoyama, T., Mem. Fac. Eng. Kyoto Univ., 17,253 (1955)

O1 O'Connell, F.P., and Mack, D.E., Chem. Eng. Progr., 46,358 (1950)

O2 Olney, R.B., and Carlsen, G. J., Chem. Eng. Progr., 43,467 (1947)

R1 Rea, H.E., Jr., and Vermeulen, T., Effect of Baffling and Impeller Geometry on Interfacial Area in Agitated Two-Phase Liquid Systems (M.S. Thesis), Lawrence Radiation Laboratory Report UCRL-2123, April 3, 1953 (unpublished)

R2 Rushton, J.H., Costich, E.W., and Everett, H.J., Chem. Eng. Progr., 46,395,467 (1950)

S1 Shinnar, R., and Church, J.M., Ind. Eng.Chem. 52,253 (1960)

T1 Taylor, J.S., Flow Patterns in Agitated Vessels (M.S. Thesis), University of Delaware, Newark, Delaware, 1955 (unpublished)

W1 White, A.M., Brenner, E., Phillips, G.A., and Morrison, M.S., Trans. A.I.Ch.E., 30,570,585 (1934)

TECHNICAL INFORMATION DIVISION
LAWRENCE RADIATION LABORATORY
UNIVERSITY OF CALIFORNIA
BERKELEY, CALIFORNIA 94720